Front. Struct. Civ. Eng. 2023, 17(1): 53–77
https://doi.org/10.1007/s11709-022-0850-0

REVIEW

Behaviour of self-centring shear walls——A state of the art review

Mehdi JAVADI, Reza HASSANLI*, Md Mizanur RAHMAN, Md Rajibul KARIM

UniSA STEM, University of South Australia, Adelaide 5095, Australia
**Corresponding author. E-mail: Reza.Hassanli@unisa.edu.au*

ABSTRACT The application of unbonded post-tensioning (PT) in structural walls has led to the development of advanced self-centring (rocking) shear wall systems that has significant advantages, including accelerated construction due to the incorporation of prefabricated elements and segmental construction for different materials (e.g., concrete, masonry, and timber), reduced residual drifts, and little damage upon extreme seismic and wind loads. Concrete, masonry, and timber are often used for the construction of unbonded PT structural wall systems. Despite extensive research since the 1980s, there are no well-established design guidelines available on the shear wall configuration with the required energy dissipation system, joint's locations and acceptance criteria for shear sliding, confinement, seismic performance factors, PT loss, PT force range and residual drifts of shear walls subjected to lateral loads. In this research a comprehensive state-of-the-art literature review was performed on self-centring shear wall system. An extensive study was carried out to collect a database of 100 concrete, masonry, and self-centring shear wall tests from the literature. The established database was then used to review shear walls' configurations, material, and components to benchmark requirements applicable for design purposes. The behaviour of concrete, masonry and timber shear walls were compared and critically analysed. The general behaviour, force-displacement performance of the walls, ductility, and seismic response factors, were critically reviewed and analysed for different self-centring wall systems to understand the effect of different parameters including configurations of the walls, material used for construction of the wall (concrete, masonry, timber) and axial stress ratio. The outcome of this research can be used to better understand the behaviour of self-centring wall system in order to develop design guidelines for such walls.

KEYWORDS self-centring shear walls, rocking walls, energy dissipation, seismic performance factors, PT loss, residual drift

1 Introduction

The new generation of self-centring (rocking) shears walls which are loaded in-plane are designed to have controlled joint opening at wall-footing interfaces. These structures show limited residual deformation upon loading events such as earthquakes which are repairable with minimal cost [1]. The controlled joint opening also helps the wall to provide a higher ductility which results in a reduced shear and flexural demand on the wall due to seismic loads [2]. Rocking shear walls accommodate displacement ductility demands by allowing for a concentrated gap to open between the wall and foundation interface instead of allowing for the development of plastic hinges as in shear walls with monolithic (fixed based) connection [3]. Rocking shear walls require much less invasive post-earthquake repairs and thus can significantly reduce repair costs [4].

Rocking systems are commonly constructed using dry joint between elements and vertical unbonded post-tensioning (PT) reinforcement. As there is no bond between the concrete and PT reinforcement, the damages are expected to be formed in the wall-footing interface only when the wall is subject to in-plane seismic loads. This is due to the rocking behaviour with a high drift capacity that causes localised damage [5]. Additionally, the rocking shear walls return to their original vertical alignment after the lateral load is removed (e.g., self-

Article history: Received Jul 12, 2021; Accepted Apr 7, 2022

centre) if adequate PT force remains in the reinforcement [6]. Furthermore, there is no strain compatibility between PT reinforcement and surrounding material (concrete, masonry, or timber). Thus, the elongation of the reinforcement is distributed along its length [7]. Unlike bonded PT, there are no localised strain in the unbonded scenario. This results in a lower level of strains in the reinforcement for which elongation is distributed over the unbonded length of the PT reinforcement.

Despite the abovementioned advantages of rocking systems, excessive deformation/drift of the rocking walls subject to lateral loads such as earthquakes and winds are considered as a major drawback of the structural system. Moreover, these walls have a limited energy dissipation (ED) capacity compared to conventional walls to address this deficiency.

1.1 Historical application of clamping methods for structural stability

Application of clamping techniques for structural stability has been well used in historical constructions. The architects of antiquity working in the medium of stone where there was no mortar used, wooden or metal clamps were used to ascertain the position of the blocks and their stability. This is an age-old technique, first known in the Old Kingdom of Egypt [8]. Later, it was used in Aegean Bronze Age architecture and in Asia Minor, Syria, and Mesopotamia. Egypt, archaic Greece and contemporary Achaemenid Persia were the first to use clamps to any greater extent. The clamps had a shape of a double dove tail, as shown in Fig. 1(a). Molten metal was poured into the cutting, and the resulting clamp was thus enforced by two or more vertical pegs [8] acting as a prestressing force when the metal cooled. The other historical application of metal clamps to hold the structural components was the use of steel in masonry structures, as shown in Figs. 1(b) and 1(c). They were mainly used to resist lateral forces, i.e., earthquakes [9].

The modern development of prestressing occurred in 1930s and is attributed to Eugene Freyssinet [10]. This allowed the application of concrete structures to larger spans competing with steel structures [9]. PT application in buildings was first applied to concrete structural elements through the PRESSS experimental program investigating five-story building constructed out of precast concrete elements [11]. The non-emulative (jointed) connection between the foundation and wall was first tested in this experiment. One of the first studies on the response of rigid rocking block on free vibration dates

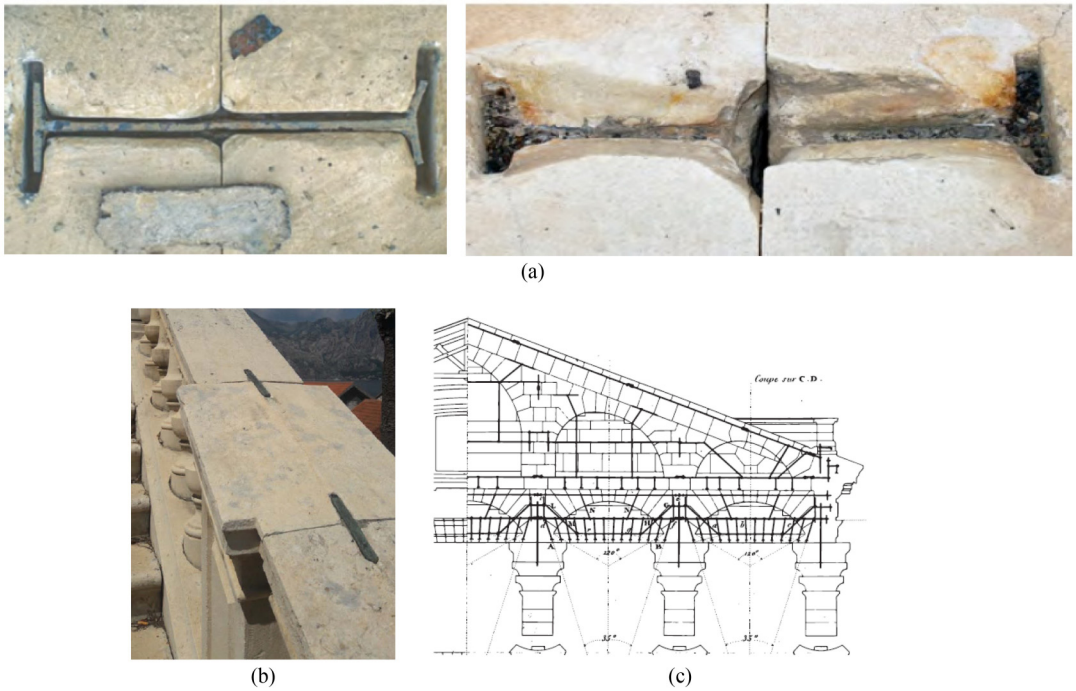

Fig. 1 History of prestressing and metallic claps in structures: (a) ancient metal clamps discovered on megaliths, temples and other prehistoric monuments worldwide adapted with permission from Kyritsis-Spinoulas et al. [12]; (b) clamps connecting two adjoined stone blocks adapted with permission from Roca et al. [9] (Reprinted from Taylor and Francis Group LLC (Books) US, Roca P, Lourenço P B, Gaetani A, Historic Construction and Conservation: Materials, Systems and Damage, 122, Copyright 2019. Reproduced with permission of the Licensor through PLSclear.); (c) Rondelet's drawings of iron tie rods and clamps in the façade of Pantheon in Paris (1756) adapted with permission from Roca et al. [9] (Reprinted from Taylor and Francis Group LLC (Books) US, Roca P, Lourenço P B, Gaetani A, Historic Construction and Conservation: Materials, Systems and Damage, 122, Copyright 2019. Reproduced with permission of The Licensor through PLSclear.)

back to nearly 50 years ago [13]. Although current retrofitting codes [14] allow for dynamic analysis of structures that freely rock on their foundation and there is a good understanding of rocking behaviour at foundation/soil interaction, this study is more focused on understanding the controlled rocking behaviour of blocks (concrete, masonry and timber) post-tensioned to a rigid foundation [15–17]. This paper also discusses the behavioural differences of rocking shear walls when constructed with different material, e.g., concrete, masonry, and timber.

1.2 Design codes

Unlike concrete, there are no well-established design codes for masonry and timber self-centring shear walls. Kurama et al. [18] has recently reviewed the advances in precast concrete related to structural rocking shear walls, which include code developments [19–21] and applications. Many jurisdictions allow performance-based seismic design (PBSD) using non-linear time history (NLTH) analysis to meet performance criteria as in FEMA P695 [22].

FEMA P695 study is usually used to evaluate period (T), and the seismic performance factors, including displacement amplification factor (C_d) and response modification factor (R) for new structural systems, which then can be used in building codes. This type of study is resource-intensive due to the extent of the NLTH analyses required. Therefore, many newly developed structural systems, such as self-centring rocking walls, do not have well-established seismic response factors in building codes [2]. Questions remain on how to solve period-stiffness dependency, provide simple design equations, and proceed in cases of hybrid systems with subsystems characterised by different plastic behaviour [23].

1.3 Concrete post-tensioned walls experimental database critical analysis and review

As part of this study, a database of 62 tested concrete rocking walls backbone curves was established and critically analysed to develop an empirical correlation between wall height and its period. Moreover, the R-factor is related to the period (T) and ductility (μ) of rocking walls which is often treated as a constant in current concrete design codes. Seismic response modification factors for masonry and timber rocking shear walls are also reviewed based on published information, and recommendations were provided for implementation in building codes.

1.4 Masonry post-tensioned walls

The applicability of controlled rocking seismic resisting systems is not limited to concrete only and can be applied in masonry also. In masonry construction, the necessity of incorporating highly skilled labours, use of mortar, cast in-situ construction method often puts a heavy burden on project costs [24]. The use of PT in masonry is promising as it can potentially reduce the cost [25].

The application of PT in masonry walls has been considered both for in-plane and out-of-plane loading. Out-of-plane loading studies include application of PT in masonry retaining walls and subject the wall to the out-of-plane loading [26–29]. There have been very limited studies on the engineering behaviour of the out-of-plane PT masonry walls [30]. The investigations were mostly qualitative and focused on wall performance in non-seismic areas under monotonic loading and were based on the review done by Lissel et al. [31] on masonry.

There have been a few studies investigating the flexural strength of a PT masonry wall resisting out-of-plane loads [32–36]. To the authors' best knowledge, all the literature on the masonry PT walls subject to out-of-plane loading had mortar in the joints of the masonry blocks. However, the experiments presented in Sokairge et al. [25] and Kohail et al. [37] did not have mortar between the masonry block joints (dry joints). The in-plane behaviour of PT masonry walls [38–43] is the focus of this review.

1.5 Timber post-tensioned walls

The self-centring concept for walls with single or multiple segments has also been developed and applied in rocking timber shear walls [44–49]. The shear walls were mainly made of laminated Veneer Lumber (LVL) or glulam timber as the primary lateral load resisting system [50]. Smith et al. [50] estimated that a building with timber self-centring lateral load resisting systems and structural frames costs only 5% more than the concrete alternative. Still, in many cases, timber can be the material of choice because of its reduced weight and lower energy (40% lower) and carbon footprint (70% lower) compared to concrete [51].

1.6 Rocking walls configurations

All rocking shear walls (concrete, masonry, and timber) behave similarly. They all self-centre, have unbonded PT reinforcement and dry joint connection in the wall-footing interface. However, they may have different wall panels configuration, material confinement at wall toe, wall panel's joint locations and ED devices. In this paper, concrete, masonry, and timber wall assembled configurations are compared, and wall toe confinement requirements (type, length, location) is discussed. Considering the larger database available for concrete rocking walls, the seismic response factors for this material is critically reviewed and compared to code presented values. The

seismic response factors for the masonry and timber rocking walls are reviewed only based on the available literature. The correlations developed for concrete in this paper for the period, and seismic response factors can also be modified for masonry and timber.

ED devices for each wall material are reviewed, and recommendations are provided suitable for design guides. Currently, available design codes for rocking shear walls do not specify acceptable limits for PT force loss and residual drifts. PT force loss and residual drifts for the collected walls database are reviewed, and an acceptance criterion is defined to be applicable in PBSD.

2 Unbonded post-tensioned shear walls tested configurations, materials, and components

Different wall configurations and material (concrete, masonry, and timber) with different components have been tested and reported in past studies to investigate the effect of confinement, wall joint behaviour, and ED.

Figure 2 shows the number of publications (searched through Scopus) on concrete, masonry, and timber rocking shear walls during the last decade. Among common construction materials considered, concrete has attracted the most research effort in PT wall application. This is probably due to the maturity of the material in the construction industry. Timber PT shear walls application in timber structures has also been considered in this review [2,44,52–54].

The next section discusses the tested wall configurations and components of wall assembly for different materials.

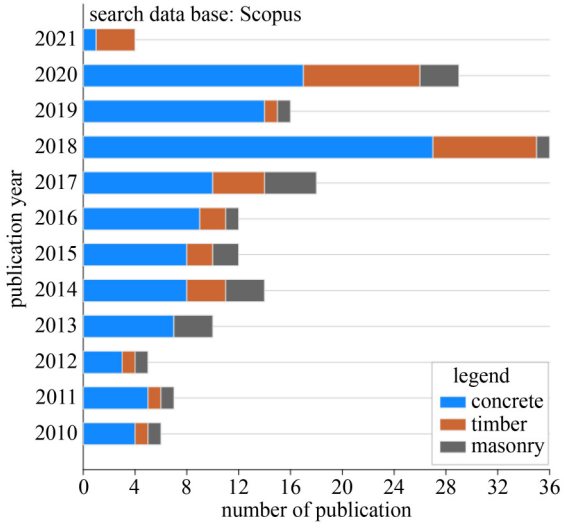

Fig. 2 Number of publications for concrete, masonry, and timber PT walls in the last decade.

2.1 Concrete post-tensioned shear walls

Figure 3 shows the different configurations of tested concrete self-centring shear walls. Some wall specimens comprise single precast wall panels [18] as shown in Figs. 3(a), 3(e), 3(g) and some include multiple panels with horizontal or vertical joints [55–58] as shown in Figs. 3(b), 3(c), 3(d), 3(f), 3(h). They all include precast wall panels with a joint at the wall-footing interface and unbonded post-tensioned rods which clamps the wall to its foundation. Table A1 in Electronic Supplementary Material presents the values for the seismic factors in respect to axial stress ratio (ASR) and aspect ratio (AR) of the tested walls. The full list of concrete self-centring shear walls that include confinement at the wall toe is tabulated in Table A2 in Supplementary Material. The confinement is introduced by either reinforcement or steel jackets at the wall base. Concrete confinement at the wall toe makes the shear wall more resilient to local failure at the wall base where there is maximum compressive stress.

Concrete confinement achieved by reinforcement, has two forms, i.e., base channels and rebars, including spirals, and ties. Therefore, concrete confinement can be treated as a function of the forms and amount of reinforcement used. Crushing of the confined concrete using spiral and tied reinforcement occurs at an ultimate concrete compressive strain and at the compressive strain of 0.004, respectively [15]. Premature failure of the base may significantly reduce the lateral strength of the unbonded post-tensioned shear walls and occurs when the wall base is not adequately confined. Kurama et al. [15] used two layers of spirals and a minimum volumetric confinement reinforcement ratio of 1.83% to tackle premature failure. The amount of spiral reinforcement within the range of 1.83% to 7.33% did not affect the lateral load capacity of the wall. This suggested that increasing reinforcement beyond 1.83% did not increase toe compressive capacity due to lower effect of confinement on the compressive strength at a very large reinforcement ratio. Holden et al. [59] and Gu et al. [57] made similar observations. Smith and Kurama [60] reported that misalignment of the confinement hoops could also be responsible for premature failure of the wall base used a 1.87% volumetric confinement reinforcement ratio, and no premature failure at wall toe was reported.

Nazari et al. [61] provided confinement at wall base using base channels having $0.20l_w$ length (l_w is length of the wall) and hoops which resulted in acceptable wall toe performance against dynamic loads. Twigden et al. [62] and Yang and Lu [63] used the concrete confinement model in Mander et al. [64] to provide confinement at the wall base. Twigden et al. [62] also used additional cast in steel angles to provide confinement and prevent toe concrete damage. Only a minor amount of spalling was observed in the wall toes at drifts greater than 2%, and no

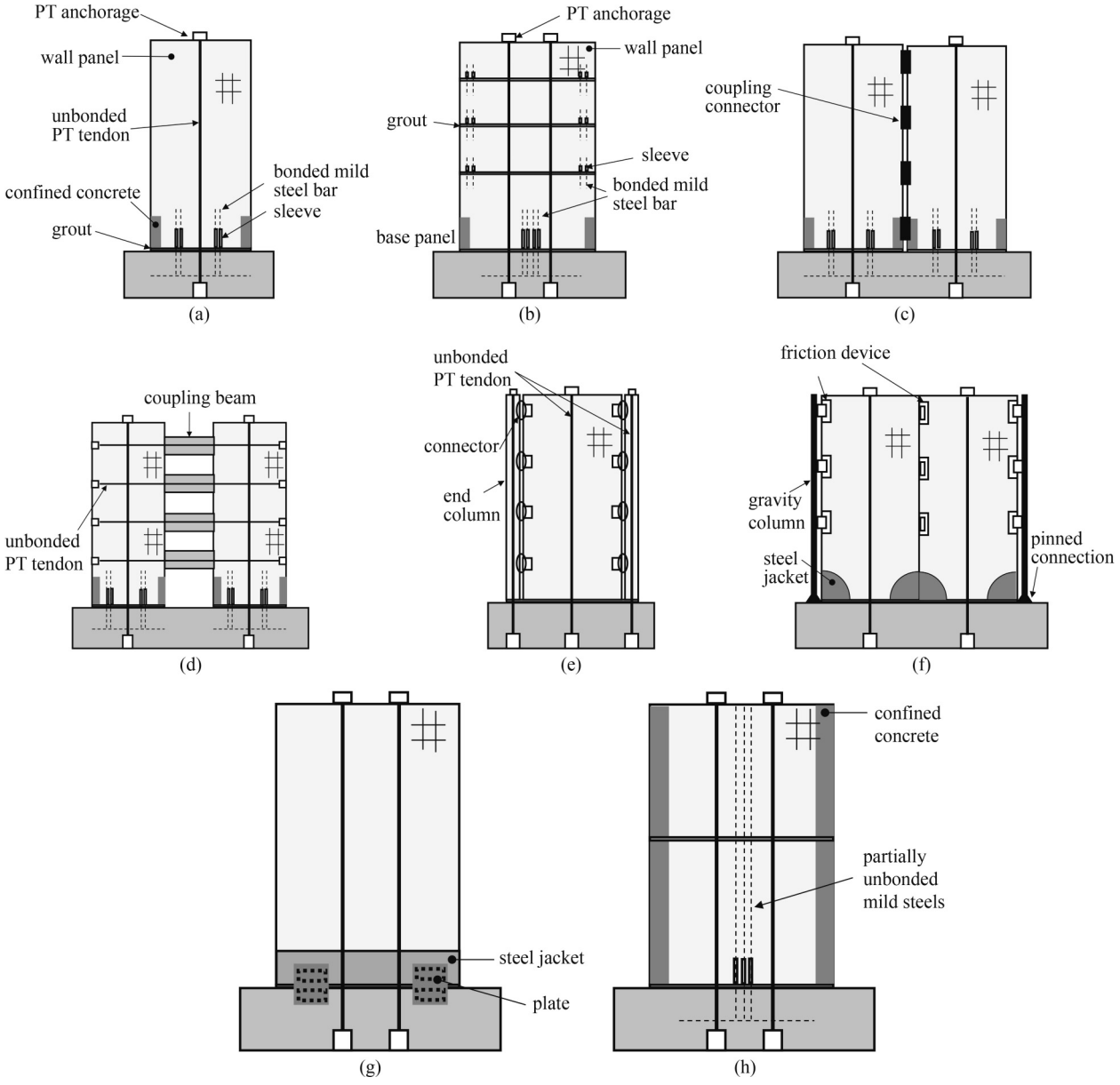

Fig. 3 Precast concrete walls configurations: (a) single panel wall adapted from Kurama et al. [18] (Used with permission of American Society of Civil Engineers, from Seismic-resistant precast concrete structures: State of the art, Kurama Y C, Sritharan S, Fleischman R B, Restrepo J I, Henry R S, Cleland N M, Ghosh S K, Bonelli P, 144, 4, 2018, permission conveyed through Copyright Clearance Center, Inc.); (b) multipaneled wall adapted from Kurama et al. [18] (Used with permission of American Society of Civil Engineers, from Seismic-resistant precast concrete structures: state of the art, Kurama Y C, Sritharan S, Fleischman R B, Restrepo J I, Henry R S, Cleland N M, Ghosh S K, Bonelli P, 144, 4, 2018, permission conveyed through Copyright Clearance Center, Inc.); (c) coupled wall with vertical joint adapted from Kurama et al. [18] (Used with permission of American Society of Civil Engineers, from Seismic-resistant precast concrete structures: state of the art, Kurama Y C, Sritharan S, Fleischman R B, Restrepo J I, Henry R S, Cleland N M, Ghosh S K, Bonelli P, 144, 4, 2018, permission conveyed through Copyright Clearance Center, Inc.); (d) coupled wall with coupling beams adapted from Kurama et al. [18] (Used with permission of American Society of Civil Engineers, from Seismic-resistant precast concrete structures: state of the art, Kurama Y C, Sritharan S, Fleischman R B, Restrepo J I, Henry R S, Cleland N M, Ghosh S K, Bonelli P, 144, 4, 2018, permission conveyed through Copyright Clearance Center, Inc.); (e) precast walls with end columns (preWEC) adapted from Henry et al. [55] (Reprinted from Engineering Structures, 115, Henry R S, Sritharan S, Ingham J M, Finite element analysis of the PreWEC self-centering concrete wall system, 28–41, Copyright 2016, with permission from Elsevier.); (f) coupled walls with friction devices adapted from Guo et al. [56] (Used with permission of American Society of Civil Engineers, from Seismic resilience upgrade of rc frame building using self-centering concrete walls with distributed friction devices, Guo T, Xu Z, Song L, Wang L, Zhang Z, 143, 12, 2017, permission conveyed through Copyright Clearance Center, Inc.); (g) repairable precast concrete shear wall; (h) hybrid reinforced shear wall adapted from Gu et al. [57] (Reprinted from Soil Dynamics and Earthquake Engineering, 116, Gu A, Zhou Y, Xiao Y, Li Q, Qu G, Experimental study and parameter analysis on the seismic performance of self-centering hybrid reinforced concrete shear walls, 409–420, Copyright 2019, with permission from Elsevier.).

bending of the steel angle was observed.

The other parameter influencing the premature failure of the wall toe is the confinement length. Table 1 summarizes the confinement lengths applied in experimentally tested walls with hoops and spirals and shows that walls produced acceptable performances with a minimum confinement length of $0.08l_w$ along the wall's length at the edges, and $0.40l_w$ along the wall's height, respectively. Based on these test results, it is recommended to use a minimum of around 2.0% volumetric confinement reinforcement ratio at the wall's base to prevent premature failures.

Wall joints in tested walls have been horizontal to account for multiple stories as shown in Figs. 3(b) and 3(h) or vertical to increase wall AR as shown in Figs. 3(c) and 3(f). AR of the wall is defined as the ratio of the height to the wall length. Coupling beams have also been tested to connect two precast wall panels, as shown in Fig. 3(d). All tested concrete self-centring shear walls included energy dissipating bars at their joints except the configurations shown in Figs. 3(e) and 3(f). PT concrete walls are designed to have controlled rocking and the gap opening, which is only allowed in the joint between the foundations. A review on the wall joints connection to floors can be found in Masrom and Hayati [65].

Shear slip can be unfavourable and must be avoided [66] in such structural systems as it damages the mild steel and consequently affect the ED and residual displacement of the system [3]. Although shear slip between the wall panel and foundation would be avoided if the wall AR is larger than 1.5 [59,66], New Zealand standard NZS 3101 [67] requires shear dowels to be placed across the joints at the base of all PT concrete walls. The horizontal slip for PT concrete walls is also limited to 1.5 mm [68]. Jafari et al. [69] mentioned the application of steel tubular elements as shear keys effectively reduces the shear sliding at the bottom of PT concrete walls. Yang and Lu [66] suggested a mathematical formula to control sliding shear at the wall base. The Wall AR should be greater than 1.54 to avoid shear sliding. Yang and Lu [66] argued that walls having ARs larger than 2.0 should not suffer from shear sliding.

ED bars at the wall-footing interface are designed to yield when the joint between the wall-footing interfaces opens. External ductile dissipative devices act as fuses that deform inelastically in case of an earthquake and can be easily replaced if damaged. This works for the economy of the building and reduces the downtime period of the structure. The connectors, as shown in Fig. 3(e) can also provide the system with hysteric ED [1]. Different types of ED devices have been investigated, including viscous dampers [70], friction devices [56–71], and mild steel O-connectors [55] (O-connectors can be used as fuses which would be easily replaced in case of an earthquake incident mitigating damage to main structural components). The area enclosed by the hysteresis loop for a cycle divided by the area of the circumscribing parallelogram in a force-displacement diagram is defined as the relative ED ratio (β) [61]. The ED ratio (β) is required to have a minimum value of 12.5% [20], which is equivalent to about 8% viscous damping [61].

Self-centring structures, especially those with replaceable energy-dissipating elements, as shown in Figs. 3(e)–3(g) achieves higher performance goals compared to traditional lateral-force-resisting systems [3]. Unbonded PT concrete walls without ED devices can have about 5.7% total equivalent viscous damping (EVD) for drift cycles larger than 1% [61]. EVD includes two components: the first is viscous damping (ξ_v), and the second is hysteresis damping (ξ_{hyst}).

$$\xi_{eq} = \xi_v + \xi_{hyst}. \quad (1)$$

The viscous damping for PT walls is small (approximately 3%) [72]. Nazari et al. [61] stated that the energy dissipated due to rocking was ignored in previous experimental studies because they were conducted primarily using quasi-static loading, and increasing the ASR would result in higher ED. However, comparison of single rocking walls designated as SRW-A tested by Twigden and Henry [73] on a shake table and SRW-B tested by Twigden et al. [62] using quasi-static load indicates that changing load on the wall from quasi-static to dynamic load leads to a decrease in EVD. SRW-B test reported 4.7% EVD at 2% drift, and SRW-A had 3.62% EVD on average.

The equivalent viscous damping (ξ_{eq}) of unbonded PT concrete walls from the different experimental investigation are summarized in Fig. 4. It shows that walls with end columns [74] (e.g., Fig. 3(e)) and hybrid precast concrete walls [75] (e.g., Fig. 3(b)) which use energy dissipating bars can be suitable for highly seismic prone areas. The PreWEC walls tested by Twigden and Henry [73] and Twigden et al. [62] were similar in geometry and configuration and tested under quasi-static and dynamic load, respectively. The preWEC system or uncoupled hybrid PT concrete walls is argued to be more effective in resisting lateral loads due to maximised wall panel length, which results in a larger moment arm in comparison to multi-panel walls having vertical joints [18]. It can be

Table 1 Reported confinement length of walls in the experimental tests

confinement length	tested wall reference
$0.08l_w$ above wall base	[15]
$0.25l_w$ on each side of centerline and $0.65l_w$ above wall base	[76]
$0.09l_w$ on each side of centerline and $0.40l_w$ above wall base	[61]
$0.08l_w$ on each side of centerline and $0.67l_w$ above wall base	[62]

Note: l_w: wall length.

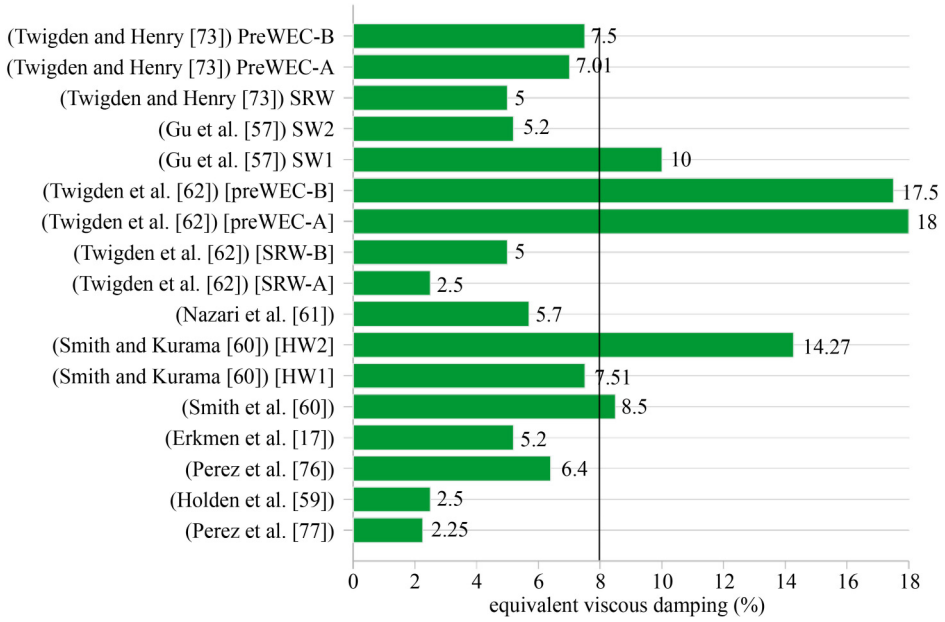

Fig. 4 EVD of unbonded PT concrete walls.

observed in the preWEC walls that the EVD in dynamic load closer to the actual earthquake load is reported at about 7.5%. However, the EVD is about 18% in quasi-static loading. The tested walls that have near 8% EVD or higher are acceptable according to ACI ITG-5.1-07 2008 design criteria.

The application of ED devices like mild steel may cause out-of-plane damages if not designed to yield in compression or in-plane shear slip [78]. It also increases residual displacements in PT concrete walls [17]. Thus, it is recommended to use a mild steel moment ratio (κ_d) from 0.5 to 0.8 [3,66,79] to satisfy ED requirement and avoid out-of-plane or in-plane residual damages. The mild steel moment ratio is defined as the moment contribution of mild steel divided by the sum of moment contribution of PT strands and gravity loads to resist lateral loads. Non-linear response history analysis on hybrid precast concrete walls [79] suggested that walls with $\kappa_d = 0.5$ results in larger base shear forces (by about 5%) in comparison to walls with $\kappa_d = 0.8$.

For one way structural walls, minimum of two modules having the configuration of Fig. 3(b) and for coupled walls, two modules with the configuration of either Figs. 3(c) or 3(d) must be tested [20] and meet the acceptance criteria for drift and minimum ED based on defined cyclic load [78]. These mandatory test configurations are required for structures in high seismic risk, or the structures designed for high seismic performance levels or design categories.

To recapitulate, a minimum confinement length of $0.08l_w$ and $0.40l_w$ and a minimum of 1.87% volumetric confinement reinforcement ratio at the wall base is required to prevent premature failure of the concrete rocking shear wall. The horizontal deflection for a shear slip at the wall base is recommended to be limited to 1.5 mm and maintain wall AR larger than 2. EVD is highly dependent on the load type acting on the wall, whether it is quasi-static or dynamic. Mild steel moment ratio is recommended to be adopted from 0.5 to 0.8 for concrete rocking shear walls.

2.2 Masonry post-tensioned shear walls

Masonry self-centring shear walls have been tested mainly with three different configurations in the reported experiments. A high-strength Calcium Silicate Element masonry with Thin Layer Mortar (CASIEL-TLM masonry) having rectangular and flanged section as shown in Fig. 5(a) was investigated experimentally by van der Meer et al. [80]. The wall with a T-shaped cross-section failed prematurely in shear at the web-flange interface resulting in diagonal splitting cracks in the interlocking units. Other self-centering walls configuration is mainly an unreinforced masonry block with unbonded PT tendons, as shown in Fig. 5(b) [81]. This wall configuration has shown more robust self-centering structural performance mainly due to the location of PT bars which has been distributed along wall length.

Masonry shear wall with no confinement reinforcement or armouring at wall toe showed excessive compressive strains [82]. An exception to this behaviour was a fully grouted masonry shear wall which included steel confining plates between construction joints at wall toes, as shown in Fig. 5(c) [83].

Masonry self-centering shear wall joints can experience gap opening in the interface between the wall panel and foundation. However, further investigation using wall systems with multiple rocking joints to mitigate higher

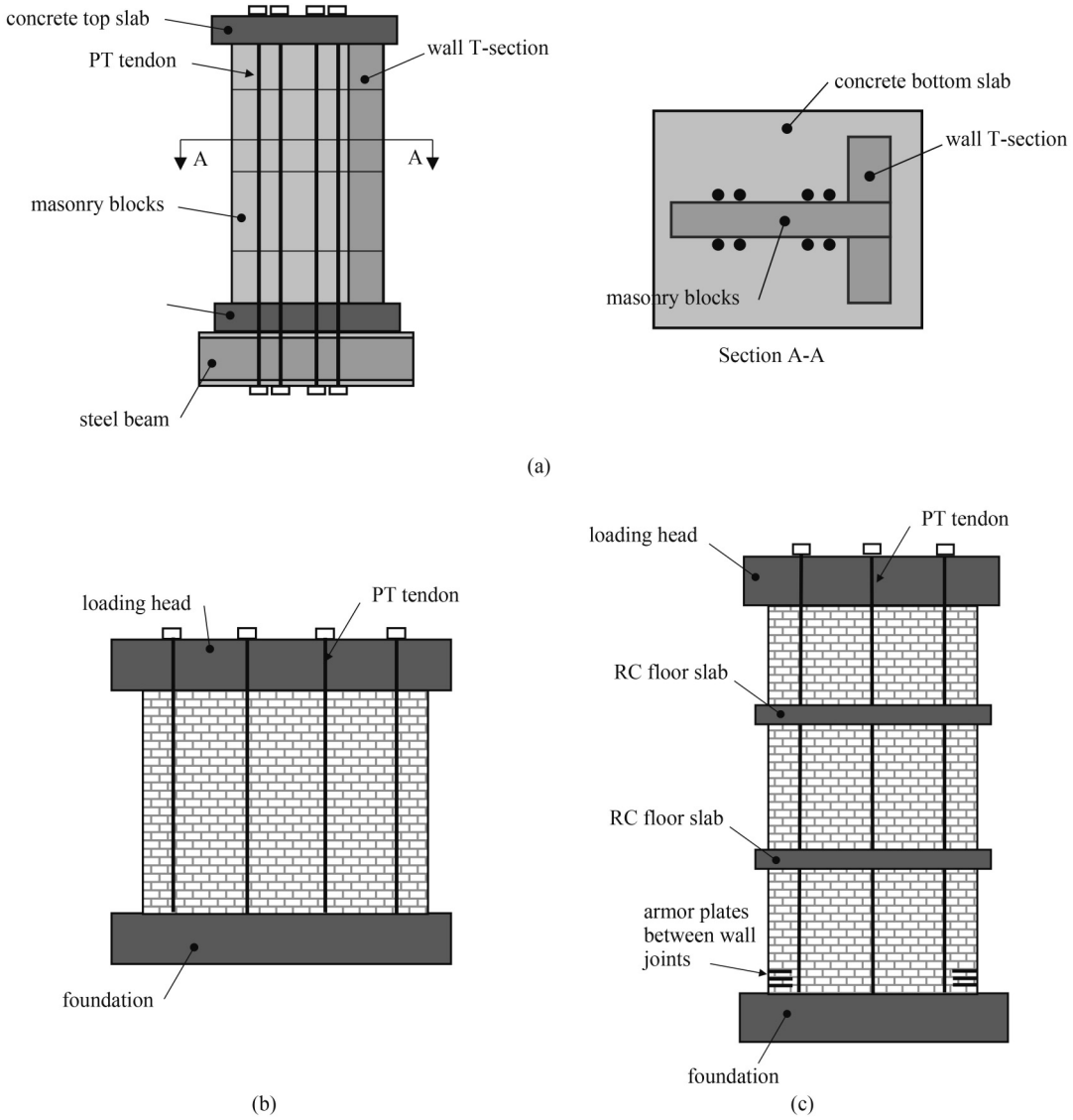

Fig. 5 Masonry PT walls: (a) high-strength Calcium Silicate Element masonry rectangular and flanged shear wall adapted from van der Meer et al. [80] (Reprinted from Engineering Structures, 49, van der Meer L J, Martens D R W, Vermeltfoort A T, UPT rectangular and flanged shear walls of high-strength CASIEL-TLM masonry: Experimental and numerical push-over analysis, 628–642, Copyright 2013, with permission from Elsevier.); (b) unbonded post-tensioned masonry shear wall adapted from Hassanli et al. [81] (Used with permission of American Society of Civil Engineers, from Experimental investigation of in-plane cyclic response of unbonded posttensioned masonry walls, Hassanli R, ElGawady M A, Mills J E, 142, 5, 2016, permission conveyed through Copyright Clearance Center, Inc.); (c) PT masonry wall with armour plates at wall toes adapted from Laursen and Ingham [83] (Used with permission of American Society of Civil Engineers, from Structural testing of large-scale posttensioned concrete masonry walls, Laursen P T, Ingham J M, 130, 10, 2004, permission conveyed through Copyright Clearance Center, Inc.).

mode effects in high rise construction (8 and 12 stories) was recommended by Yassin et al. [7]. Unlike concrete and timber rocking walls, no study has been performed to investigate the floor connection system to rocking masonry walls.

2.3 Timber post-tensioned shear walls

Timber self-centering shear walls have been tested with different configurations as shown in Fig. 6. Timber PT walls have been following a similar configuration as the concrete panels using the same ductile steel connectors and energy dissipating devices that works as structural fuses. A recent study has used aluminum O-connectors providing EVD in a range of 20% and 40% [84], as shown in Fig. 6(f). Plywood sheets as shown in Fig. 6(d), are only used in timber walls to connect two rocking wall segments together by nails. Pilon et al. [52] tested multiple rocking segments for Cross Laminated Timber (CLT) and LVL Prestressed Laminated (Pres-Lam) wall systems.

The wall configuration is shown in Fig. 6(a) [52] which

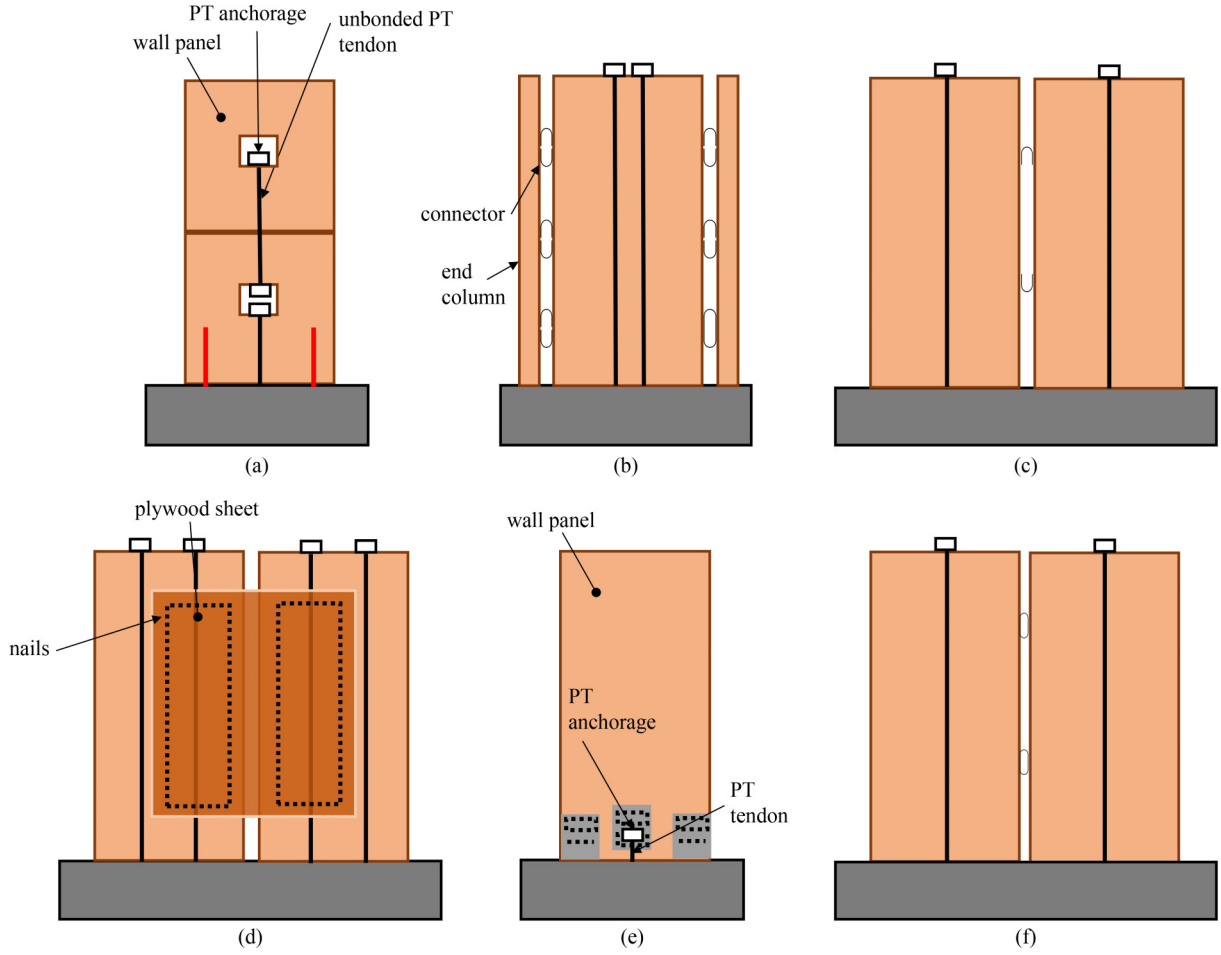

Fig. 6 PT Timber walls configurations: (a) coupled panel with horizontal joints adapted from Pilon et al. [52] (Reprinted from Soil Dynamics and Earthquake Engineering, 117, Pilon D S, Palermo A, Sarti F, Salenikovich A, Benefits of multiple rocking segments for CLT and LVL Pres-Lam wall systems, 234–244, Copyright 2019, with permission from Elsevier.); (b) panel with end columns adapted from adapted from Sarti et al. [48] (Used with permission of American Society of Civil Engineers, from Development and testing of an alternative dissipative posttensioned rocking timber wall with boundary columns, Sarti F, Palermo A, Pampanin S, 142, 4, 2016, permission conveyed through Copyright Clearance Center, Inc.); (c) U-shaped flexural plate and its application in coupled rocking LVL shear wall adapted from Moroder et al. [45] (Reprinted from Engineering Structures, 167, Moroder D, Smith T, Dunbar A, Pampanin S, Buchanan A, Seismic testing of post-tensioned Pres-Lam core walls using cross laminated timber, 639–654, Copyright 2018, with permission from Elsevier.); (d) coupled walls with vertical joint; (e) CLT with slip friction connection adapted from Fitzgerald et al. [85] (Reprinted from Engineering Structures, 220, Fitzgerald D, Miller T H, Sinha A, Nairn J A, Cross-laminated timber rocking walls with slip-friction connections, 110973, Copyright 2020, with permission from Elsevier.); (f) CLT with Aluminium O-connectors adapted from Hossain et al. [84] (Used with permission of American Society of Civil Engineers, from Experimental investigation and finite-element modeling of an aluminum energy dissipater for cross-laminated timber walls under reverse cyclic loading, Hossain K, Aaleti S, Dao T N, 147, 4, 2021, permission conveyed through Copyright Clearance Center, Inc.).

includes external dissipaters and the PT of the panels. The PT rod connecting the wall panels is separate from the rod that connects the bottom panel to the foundation. Results indicated that the CLT wall needed 20% wider panels and 10%−30% less PT force in comparison to LVL panels to obtain the same moment-rotation behaviour as in the LVL walls. Sarti et al. [48] tested timber wall panels adopting concrete wall configuration from Prestressed Walls with End Columns (PreWEC). The O-connectors used in both timber and concrete rocking walls yielded at 30 kN at 4 and 5.08 mm lateral displacement and resulted in 12.9% and 14% hysteretic damping for timber and concrete rocking wall, respectively. The experimental results confirmed the excellent seismic performance of the wall. The configuration of the tested wall like PreWEC is shown in Fig. 6(b). The U-shaped flexural plate and its application in coupled LVL shear wall is shown in Fig. 6(c) [45].

Iqbal et al. [44] tested a wall pair connected with a plywood sheet (similar to Fig. 6(d)). The experiment results indicated good self-centering performance having minimal damage with nails connecting the plywood sheet to LVL panels working as the energy dissipating devices. The damage was mainly due to the yielding of the nails, which can be replaced. Fitzgerald et al. [85] tested the CLT wall having a short post-tensioned restoring rod and

slip friction connection at wall toes. The configuration of this wall is depicted in Fig. 6(e). The Belleville springs and brass shims used in the slip friction connection provided stable slip force and damping to the structural system. Hashemi and Quenneville [86] tested CLT walls having re-centering wall toe connections but did not include PT rod. Although the rocking wall system indicated self-centering behaviour, more residual drift was observed during a test in comparison to post-tensioned wall systems. The configuration of this wall is not included as this paper only focuses on the rocking PT walls.

Among the tested configurations for timber walls as shown in Fig. 6, the ones with O-connector ED devices provided adequate ED and self-centering behaviour, and the structural system is very similar to concrete rocking walls. A more simplistic ED system with adequate performance is introduced to rocking timber walls by adding two 12 mm plywood sheets nailed to both sides of the wall, as shown in Fig. 6(d). The nail undergoes plastic deformation in cyclic loading and provides the ED required to the system. Nails are the only components that need to be replaced after structural damage due to an earthquake which is an easier process compared with O-connectors. The configuration proposed in Figs. 6(b)−6(e) is a rocking wall in which there is a joint opening in the wall foundation interface only, regardless of the wall height. However, the configuration shown in Fig. 6(a) introduces multiple horizontal rocking joints along with wall height (at every floor level) which reduces the moment demand on the wall by 45% [52]. The floor diagram subassembly of the timber rocking shear walls has been studied by Amer et al. [87].

Unlike concrete walls, wall toe confinement has not been investigated in timber rocking walls as no considerable damage at the wall base was observed in different studies [47]. Lin et al. [88] investigated the possibility of using a curved base for PT rocking walls as the proposed geometry reduces stress concentration at wall toes. The concept of the wall is shown in Fig. 7. The curved base at wall toe can significantly reduce the stress concentration and provide confinement to mitigate toe crushing and increase the drift at which PT yielding/rupturing occurs in comparison to rectangular walls. The curved base also introduces varying stiffness that can be used based on the magnitude of the lateral force acting on the wall.

Unlike concrete PT walls for which joint opening is restricted (allowance is only made to have a joint opening at the wall-footing interface), PT CLT rocking walls have been considered to undergo joint opening at mid-height of a prototype building model to reduce lateral earthquake demand on the shear wall [2]. Pilon et al. [52] argued that single rocking segment systems with rigid connections between panels result in a dynamic amplification of forces in the upper stories. The dynamic amplification in LVL and CLT panels can be reduced by introducing simple connections allowing a gap opening at construction joints. This study showed that shear and bending moment envelopes were reduced by 45% in comparison with an equivalent single rocking segment system.

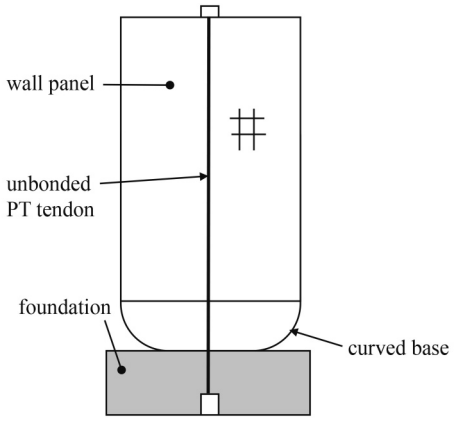

Fig. 7 Unbonded PT wall with curved base adapted from Lin et al. [88] (Reprinted from Engineering Structures, 197, Lin C P, Wiebe R, Berman J W, Analytical and numerical study of curved-base rocking walls, 109397, Copyright 2019, with permission from Elsevier.)

To develop seismic resisting systems for timber construction, different hybrid solutions for internal and external (beam-to-column, column-to-foundation or wall-to foundation) energy dissipative devices has been tested [44]. The most commonly used ED devices are U-shaped flexural plates (UFPs), tension-compression yield (TCY) elements [88] or plywood sheet coupling wall panels [44] in PT rocking timber walls. In addition to the energy dissipative devices application, allowances could be made for wall toe to be damaged for additional ED [53]. Unlike concrete shear walls, which mainly had gap openings in the wall-footing interface, the UFPs in timber walls can have a gap opening along construction joints that experienced different deflections [2]. The UFP deformation increased as it is positioned at a higher elevation along with the height of the wall below the mid-height rocking joint. Above the mid-height rocking joint, a significant drop in maximum UFP deformation was observed due to decreased flexural demands. New Zealand earthquake code NZS1170.5 [89] recommends a minimum value of $\beta = 0.55$ to provide sufficient ED and to limit residual displacement in the structure where β is the ratio of PT moment contribution to the total moment distribution in the system.

3 Review of the experimentally tested walls' seismic performance factors

In this section, the seismic performance factors and ductility of concrete walls presented in American

building codes are critically reviewed based on the collected database of force–displacement curves of experimentally tested self-centering rocking concrete shear walls. However, the performance factor and ductility of masonry and timber are only presented and discussed based on literature review and published conclusions since the number of experimentally tested timber and masonry walls may not be adequate to make a generalised conclusion considering that the results are highly dependent on the dynamic characteristics of a structure, as well as the ground motions utilised for assessment [2].

3.1 Self-centering concrete shear walls

The bilinear idealisation of backbone curves as shown in Fig. 8 has been adopted from ATC [90,91] and FEMA 356 [14] generally having elastic-perfectly plastic [92] or elastic hardening/softening [14,93] fitting rules to establish seismic performance factors including displacement ductility (μ), response modification factor (R), displacement amplification factor (C_d) [94], and fundamental period of the tested structure (T). Backbone curves of 20 experimentally tested concrete walls, as presented in Fig. 9 is used to investigate the PT concrete walls seismic performance factors.

The basis of seismic factors calculation using bilinear fitted curves can be found in Jafari et al. [69] for concrete walls. However, the equations and assumptions are presented here for completeness:

$$\mu = \delta_m/\delta_y, \tag{2}$$

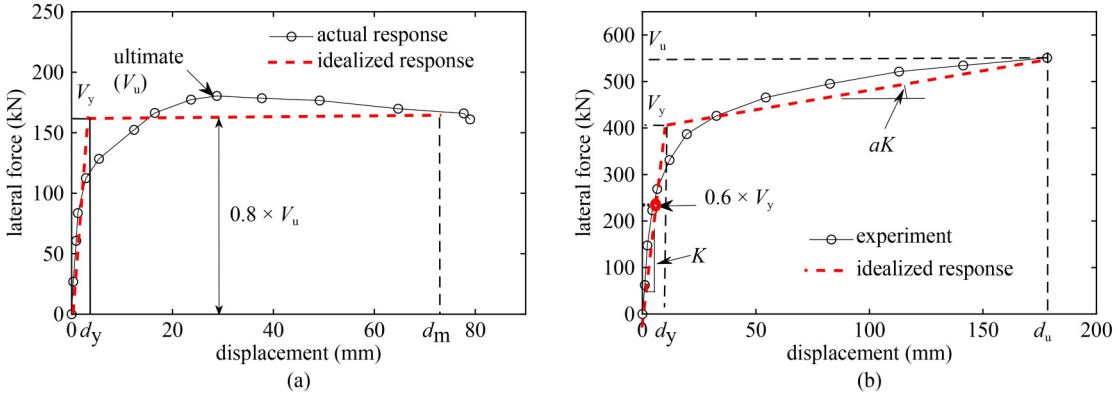

Fig. 8 Bilinear idealization: (a) ATC; (b) FEMA 356.

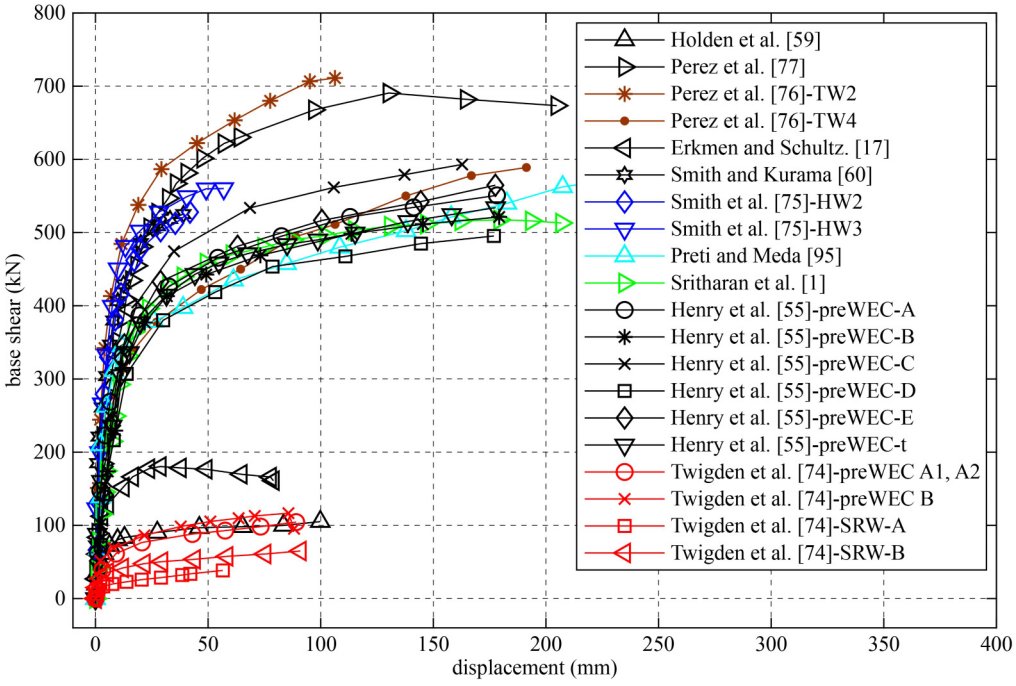

Fig. 9 Backbone curves of PT concrete walls tested experimentally.

$$R = R_R R_\mu R_s;\ R_R = 0.71;\ R_s = 1.419;$$
$$R_\mu = (\mu - 1)T/T_c + 1T < T_c, \quad (3)$$

$$T = 2\pi\sqrt{m\delta_y/V_y}, \quad (4)$$

$$C_d = \mu/\sqrt{2\mu - 1}, \quad (5)$$

where δ_m and δ_y are the maximum and yield displacements in a fitted bilinear curve, R_R is the redundancy factor recommended by ATC-19 [90], R_μ is the ductility reduction factor [96], R_s is overstrength factor [97], V_y is the base shear at yield point of the wall, T_c is characteristic period of the ground motion defined for soil types. According to ASCE 7-16 [98], T_c values changes based on site soil type. Site classes are categorised as "A", "B", "C", "D", and "E" for "hard rock", "rock", "very dense soil and soft rock", "stiff soil", and "soft clay soil", respectively. T_c can be assumed 0.52 for type "A-B", 0.75 for type "C", 0.79 for type "D", and 1.20 s for type "E" soil (refer to ASCE 7 standard for soil descriptions and shear wave velocities).

In Table 2, the average values for seismic factors for each test series and the average of all 62 PT concrete wall tests have been presented. The ductility of PT self-centering concrete walls can be seen to be different for different test series with a calculated average of 24.1. ASCE 7-16 [98] prescribes the use of a constant value for ductility of PT concrete self-centering walls.

Jafari et al. [69] and Hassanli et al. [99] argued that PT Concrete walls' ductility is highly sensitive to ASR. The choice of parameters was mainly due to limited available information in the literature suggesting correlation between ductility and axial stress ratio mainly studies by Hassanli et al. [99]. Investigating the collected database also revealed that there may be a correlation between ductility, ASR, and AR.

Jafari et al. [69] also argued that the ductility alterations become less sensitive to ASR at ASR > 0.15. A recent numerical parametric study indicated that the ASR and tendons' prestressing ratio in concrete rocking shear walls should be limited to a range of 0.075−0.115 and less than 0.75, respectively to meet basic objective performances [100] in the absence of internal/external ED mechanisms. However, plotting the experimentally tested concrete walls ductility alterations with wall AR and ASR as shown in Fig. 10(a) shows that ductility of concrete PT walls is also dependent on the wall AR which is not included in equation recommended by Hassanli et al. [99] suggesting the ductility value equal to 1.7 times the ASR. Equation (6) correlates ASR with ductility.

$$\mu = 1.7 f_p/f_c', \quad (6)$$

where f_p is the sum of stress due to self-weight and PT force, and f_c' is concrete compressive strength. The relation was developed based on a parametric numerical investigation on walls having the same AR. Wall height to width ratio between 2 and 3 tend to have different ductility variation as shown in Fig. 10(a) in comparison to walls having ARs of 1.5 or more than 3. It can also be observed that for any particular AR, ductility reduces with ASR. More study is required to account for the wall AR effect on ductility. The fundamental period, T, of all tested walls with respect to walls' heights are shown in Fig. 10(b). By increasing the wall height, the vibration period of the wall increases. Using linear regression analysis, it is possible to relate wall height to its fundamental period. The following equation is

Table 2 Average values of the seismic factors for the tested PT concrete walls

reference	ductility	T (s)	R				C_d	No. of walls
			A, B	C	D	E		
Perez et al. [77]	11.34	0.27	6.37	4.73	4.54	3.33	2.44	1
Holden et al. [59]	37.27	0.14	10.84	7.82	7.48	5.27	4.35	1
Perez et al. [76]	23.04	0.18	8.60	6.27	6.00	4.30	3.43	2
Erkmen and Schultz [17]	12.71	0.12	3.83	2.96	2.86	2.23	2.57	1
Smith and Kurama [60]	14.63	0.09	3.52	2.75	2.66	2.09	2.75	1
Henry [101]	29.44	0.09	6.40	4.75	4.56	3.34	3.74	32
Smith et al. [75]	12.85	0.11	3.49	2.73	2.64	2.08	2.58	2
Preti and Meda [95]	53.65	0.27	28.73	20.23	19.25	13.02	5.20	1
Sritharan et al. [1]	16.14	0.20	6.78	5.01	4.81	3.51	2.89	1
Henry et al. [55]	18.44	0.21	8.06	5.90	5.65	4.06	3.06	6
Twigden et al. [62]	31.15	0.13	8.61	6.28	6.01	4.30	3.96	4
Jafari et al. [69]	28.51	0.31	17.37	12.35	11.78	8.10	3.56	10
average of all tests	24.10	0.18	9.38	6.81	6.52	4.64	3.38	62

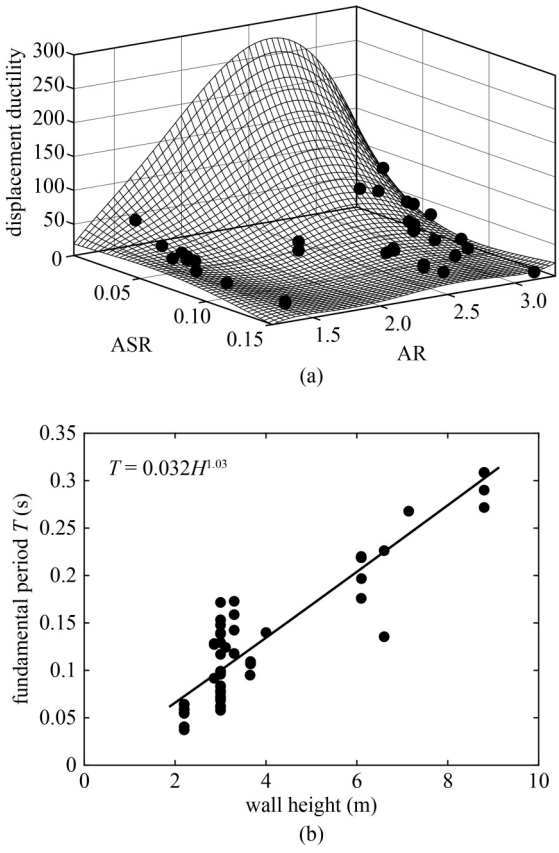

Fig. 10 Displacement ductility and wall fundamental period: (a) alterations of PT concrete walls with ASR and AR of walls (R^2 = 0.82); (b) wall height versus fundamental period of the wall.

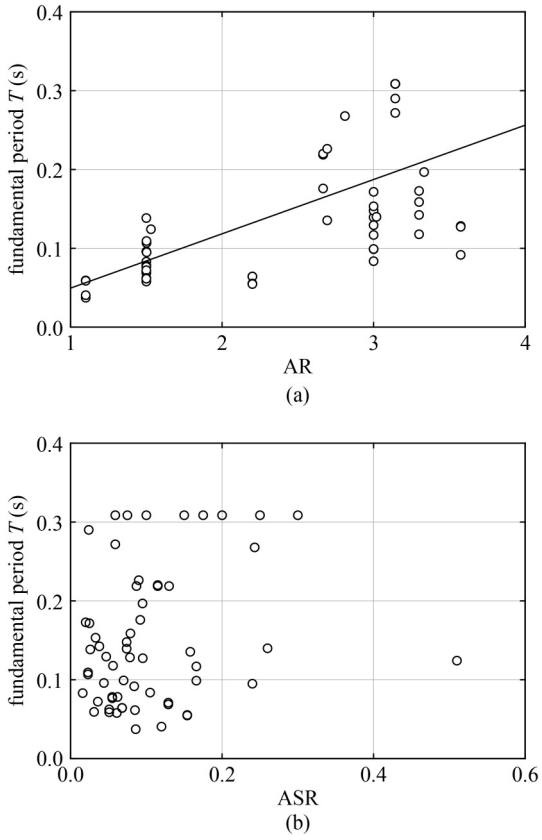

Fig. 11 (a) Fundamental period of the tested PT concrete walls versus AR; (b) fundamental period of the tested PT concrete walls versus ASR.

recommended based on the observation in this paper for calculation of fundamental period for unbonded PT concrete walls,

$$T = 0.032H^{1.03}, \quad (7)$$

where T is in seconds and H is the height of the wall in meters.

The changes in the fundamental period of PT concrete walls with ASR and AR is presented in Fig. 11. It can be seen that T increases with wall AR and a maximum value of 0.32 s was observed within the dataset collected which puts PT concrete wall in structures with low periods of less than 1.0 s [102]. This also confirms that the assumption of short period structures [94] for rocking concrete walls is valid. No clear trend was observed between ASR and T.

Response modification factor R is used to correlate ductility and ED of structures to account for the seismic forces acting on it. An increase in PT wall ductility which itself would be a function of ASR as discussed above, and wall AR results in an increase in R as the trend can be observed in Fig. 12 for two soil types having different transition period.

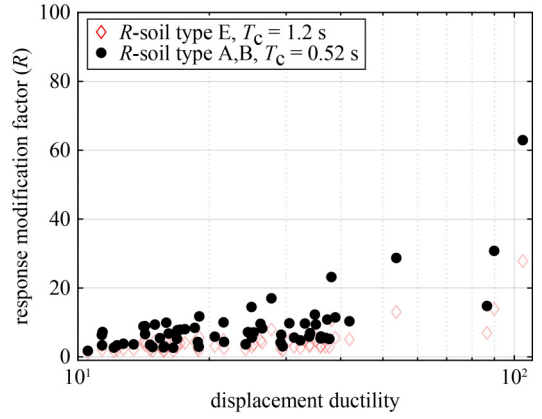

Fig. 12 Response modification factor change with ductility for soil types A, B, and E.

Figure 13 shows R-factor average values for tested wall series having different transition periods. According to ASCE 7-16 [98], R-factor for special reinforced concrete shear walls in Table 12.2.1 of the standard is 5.0 which is conservative for some tests and underestimates the R-factor in others as shown in Fig. 13. Assigning R-factor equal to 3.0 can cover all uncertainties but may increase estimated seismic load acting on the structure making the

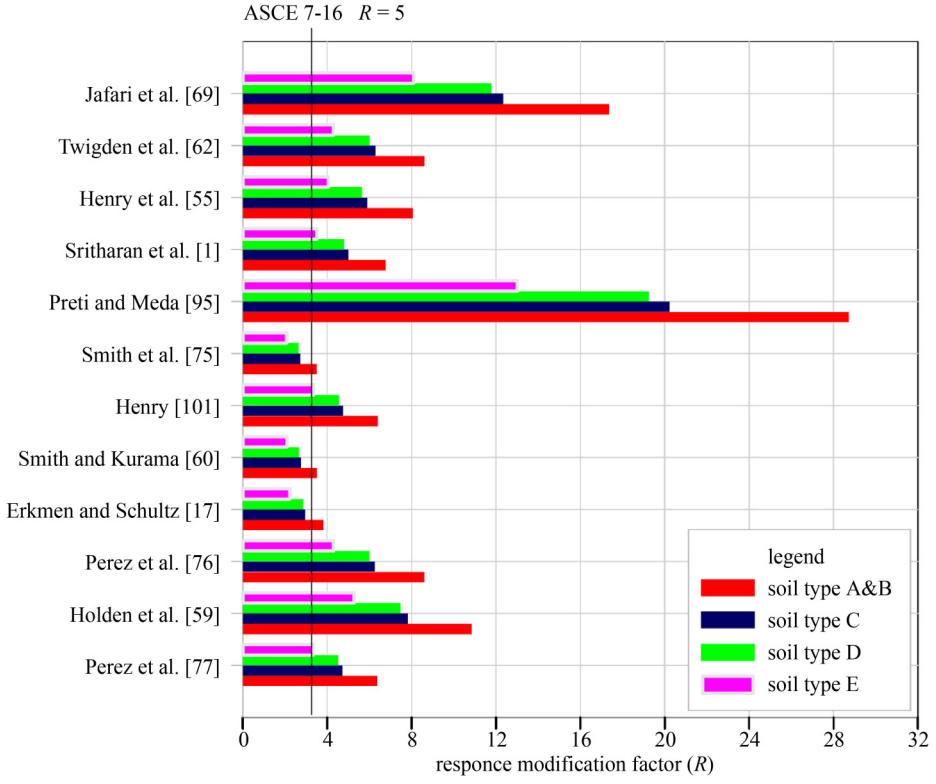

Fig. 13 Response modification factor average values for PT concrete wall test series for different soil types ASCE 7-16 [98] value for special reinforced concrete shear walls.

design uneconomical. R to soil type A, B is plotted relative to period of the tested walls and ductility as shown in Fig. 14. Considering that ductility correlated with axial stress ratio and a meaningful correlation could have been established between wall height and period, more investigation also revealed that there is a meaningful relation between R-factor, period, and ductility. It can be observed that the response modification factor, R, directly correlates with the ductility of the wall and its period as shown in Eq. (8) (Fig. 14 curve fit).

$$R = 31.9T + 0.19\mu. \tag{8}$$

Substituting Eq. (7) in Eq. (8) gives the estimated R-factor based on wall height and ASR. Equation (9) estimates R-factor using elastic period and ductility.

$$R = 1.02H^{1.03} + 0.32 f_{\mathrm{p}}/f_{\mathrm{c}}', \quad R < 9. \tag{9}$$

In addition to the effect of wall height and ASR on the response modification factor, the soil type where the structure is going to be constructed affects the response of the rocking shear wall. The R-factor against the fundamental period of the tested walls for different soil type classifications as in ASCE 7-16 [98] is reviewed. The response modification factor values scattered from 1.3 to 16.5. However, for a higher transition period (soil type E) the R-factor is less sensitive to fundamental period of the walls. Considering the sensitivity of

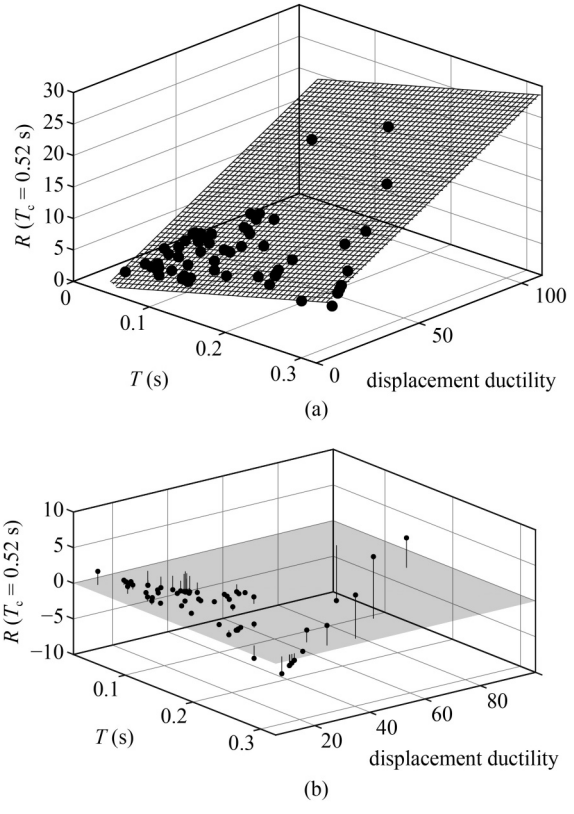

Fig. 14 (a) R-factor vs. period; (b) R-factor vs. ductility fitted surface residuals.

R-factor to elastic period, next section discusses the application of secant period to calculate *R*-factor.

The secant period of the PT self-centering walls is defined based on the ultimate displacement and force of the laterally tested wall. The plot presented in Fig. 15 illustrates the variation of *R*-factor with secant period for reviewed walls. Using the regression relationship between *R*-factor and secant period, and assuming the post-yield slope to elastic line slope ratio average equal to 0.023 extracted from the digitised force-displacement curve of tested walls, the *R*-factor estimation based on elastic period and ductility can be written.

$$T_s = 2\pi\sqrt{m\delta_u/V_u}, \tag{10}$$

$$T_s = T_i\sqrt{\mu/1+\lambda(\mu-1)}, \tag{11}$$

$$\lambda = 0.023,$$

$$R = 6.7[T^2(\mu/1+0.023(\mu-1))] + 2.9T[\mu/1+0.023(\mu-1)]^{0.5} + 3R < 7.5, \tag{12}$$

where μ is the ductility. The estimated *R*-factors versus measured ones from experiments using Eq. (9) is presented in Fig. 16(a). Large discrepancies exist for *R*-factor larger than 9.0. Thus, it is recommended to limit the upper bond of *R*-factor in Eq. (9) to 9.0. The *R*-factor using Eq. (12) is depicted in Fig. 16(b). *R*-factors estimated under 7.5 using secant period has better accuracy in comparison to elastic period through Eq. (9). The lower bond for *R*-factor is 2.0 and the upper bond is 9.0. Using *R*-factor which is estimated by the period of the wall and the ductility would result in a more realistic value for concrete PT self-centering walls.

Displacement amplification factor (C_d) is plotted against tested walls' ASRs and displacement ductility in Fig. 17. It can be seen that only three samples (out of 62) have C_d values above 5 which is recommended in ASCE 7-16 [98]. While the value of C_d = 5 appears to be reasonable for most of the samples, a value of 7.0 should be considered to provide a safe design for all the tests. Although the recommended value in ASCE 7-16 covers 95.2% of the tested specimens in this database, more parametric study is required to ensure that there is an adequate safety factor to cover all wall configurations and specifications. It is worth noting that the walls with high C_d of more than 6.5 where walls "A3" and "B1" tested and reported by Henry [101]. These walls had the lowest V_y and V_m and highest ductility among all tested walls collected in the database. This was due to the very low ASR value of (0.016−0.020) among the other walls of the test database. This indicates that walls with low shear strength and large ductility due to low levels of ASR, may result in C_d values greater than the recommended values in the code. More testing and parametric study is required to make a logical relation among the yield and

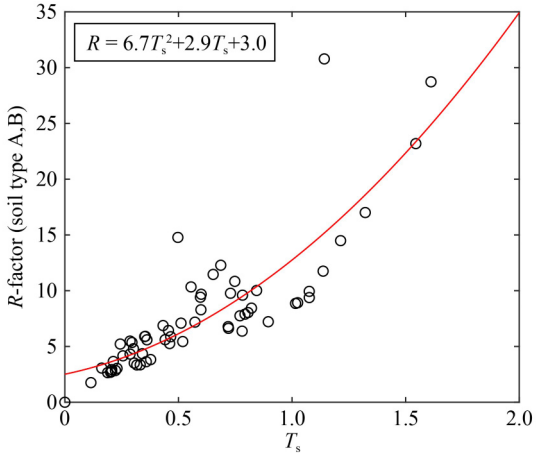

Fig. 15 *R*-factor vs. secant period of tested concrete walls.

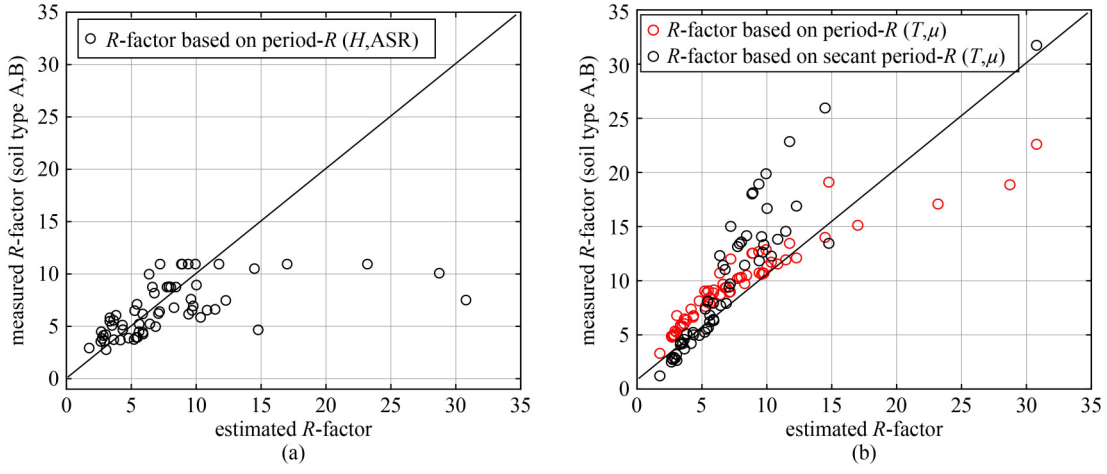

Fig. 16 (a) *R*-factors estimated by Eq. (9) where it is a function of wall height and ASR; (b) *R*-factor estimated by Eq. (12) where it is a function of elastic period and ductility.

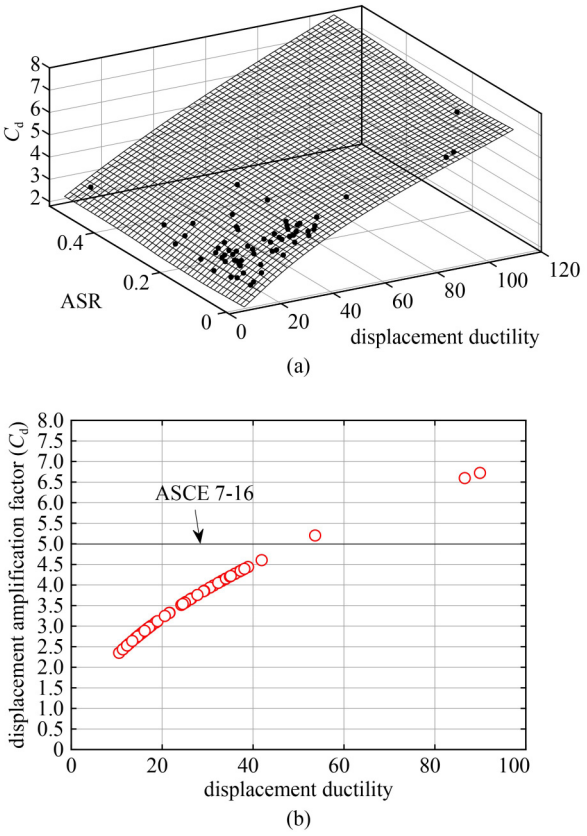

Fig. 17 (a) Displacement amplification factor (C_d) versus ASR and displacement ductility, R^2 = 0.99; (b) displacement amplification factor versus displacement ductility.

maximum shear, ductility, and ASR with C_d values. It is worthwhile to mention that most of research to date focuses on the maximum values of ASR to prevent premature failure in concrete, however, the findings indicate that a minimum value for ASR in rocking PT walls needs to be assigned to prevent large C_d values. Alternatively for low levels of ASRs, a larger value of C_d should be considered in the standards to provide a safe design.

3.2 Self-centering masonry shear walls

The research on rocking masonry walls has been limited in comparison to conventional reinforced masonry walls with fixed based connection as a seismic force resisting system [7]. As a result, no distinct seismic response factors are suggested in North American building codes and design standards for unbonded post-tensioned controlled rocking masonry walls (PT-CRMWs). Yassin et al. [7] performed a study to investigate the seismic collapse risk of fully-grouted unbonded PT-CRMWs with self-centering capacity using FEMA P695 [22] methodology. The results indicated that, R = 5.0, currently assigned to special reinforced masonry walls can meet the FEMA P695 [22] acceptance criteria for low rise buildings (2 stories) under maximin considered earthquake (MCE). For high rise masonry building construction (8 and 12 stories), the R = 5.0 did not fully meet the FEMA P695 [22] criteria due to higher mode effects. Yassin et al. [7] recommended that R = 5.0 would have passed the acceptance criteria if shear failure was prevented and confinement was provided to wall toe.

Seismic performance factors for post-tensioned (bonded/unbonded) masonry shear walls have also been studied by Hassanli et al. [42]. The R-factor value for partially grouted, fully grouted, and ungrouted post-tensioned masonry wall was recommended 2.5, 3.0, and 1.5 respectively. Displacement amplification factor (C_d) of 3.5 was suggested for fully grouted walls. However, the average values for ungrouted, partially grouted, supplemental mild steel and walls with openings were 1.8, 2.9, 4.5, and 2.6, respectively. It was also concluded that ungrouted post-tensioned masonry walls are likely to show brittle behaviour.

ASCE7 considers an R-factor of 1.5 for all types of PT masonry walls. However, Hassanli et al. [42] indicates that while an R-factor of 1.5 is reasonable for ungrouted PT masonry walls, however, it is too conservative for partially and fully grouted PT masonry walls and hence recommended R-factors of 2.5 and 3 for partially grouted and fully grouted walls respectively. Lower R-factors may result in an increased base shear FEMA P695 [22], which may not be economical for the design and construction of structures.

Tested walls included in Hassanli et al. [42] investigation did not include high rise construction and more research is required to investigate higher modes effects for high rise buildings. Yassin et al. [7] also recommended further investigation using wall systems with multiple rocking joints to tackle increased shear and flexural demand in high rise construction.

3.3 Self-centering timber shear walls

Many recently developed structural systems such as self-centering PT timber walls do not have established seismic response factors [2]. Sarti et al. [46] did an extensive parametric analysis to determine seismic performance factors for PT rocking timber shear walls according to FEMA P695 [22] procedure. The recommended seismic performance factors are as follows according to FEMA P695 [22]: Response modification factor, R = 7.0; Displacement amplification factor, C_d = 7.5; System overstrength factor, Ω_0 = 3.5.

The response modification factors can be implemented on NZS1170.5 [89] as inelastic spectrum scaling factor k_μ = 2.0.

The influence of the rocking behaviour of shear walls on the fundamental period of CLT structures has been investigated [103]. Unlike the developed equation for rocking concrete walls in this paper that correlates the

fundamental period to wall height, the fundamental period of the CLT rocking wall is correlated to geometrical slenderness, shear modulus, wall thickness and number of stories [103] and is only valid for buildings up to 5 stories. The numerical parametric study by Casagrande et al. [103] revealed that there is a significant dependency of the fundamental period of CLT structures on the ASR. No significant change in fundamental period was observed in CLT rocking walls when length of the wall and number of stories changed. This suggests that fundamental period of light weight material such as timber in rocking systems is more dependent on the ASR rather than AR.

4 Post-tensioning loss

In a structure PT may experience immediate and time-dependent PT losses. The immediate PT loss is defined as the difference between the PT force applied by the hydraulic jack on the tendon and the force in the tendon at a specific point along its length immediately after load transfer. The immediate PT losses occur mostly due to elastic shortening of concrete, draw-in at the prestressing anchorage, and friction in the hydraulic jack [104]. The time-dependent PT losses occur progressively during the life of the structure. Although creep and shrinkage are the main contributors to time-dependent PT losses, AS 3600 [105] recommends consideration of relaxation effects (due to interactions the creep, shrinkage and relaxation have with each other in measuring the PT losses) in total time-dependent losses.

The immediate losses mostly depend on the PT equipment used in construction however, the time-dependent losses mainly occur due to properties of the material used in the construction of a structure. Holden et al. [59] proposed that the use of carbon fibre tendons that behaves linearly till failure may significantly reduce stress losses due to shrinkage and creep.

To avoid overstressing during PT, AS 3600 [105] requires limiting the maximum PT force to $0.75 f_{ub} A_p$ where f_{ub} is the breaking stress of PT tendons, and A_p is the tendon cross section area. All the experimentally tested concrete walls (from literature) met this criterion as shown in Fig. 18. Approximately 4 in 5 of the tested walls suffered maximum PT losses (approximately 30%) in the ultimate state, and all tested walls had a stress ratio equal to or less than 25% with one exception [17]. Erkmen and Schultz [17] has considered the contribution of PT force and wall self-weight approximate equal to 25%, however, they have included additional weight on top of the wall to account for upper stories weight acting on the wall which increased the overall ASR to 50%. Due to high ASR, the test has experienced 100% PT loss. Although PT concrete walls still have their self-centering characteristics even after total loss of PT forces [61], it would be conservative to consider 30% PT forces loss in the ultimate state of the wall excluding immediate and time-dependent stress losses.

Table A2 in Electronic Supplementary Material includes a list of masonry walls tested experimentally. Only the masonry PT walls that reported the PT losses are

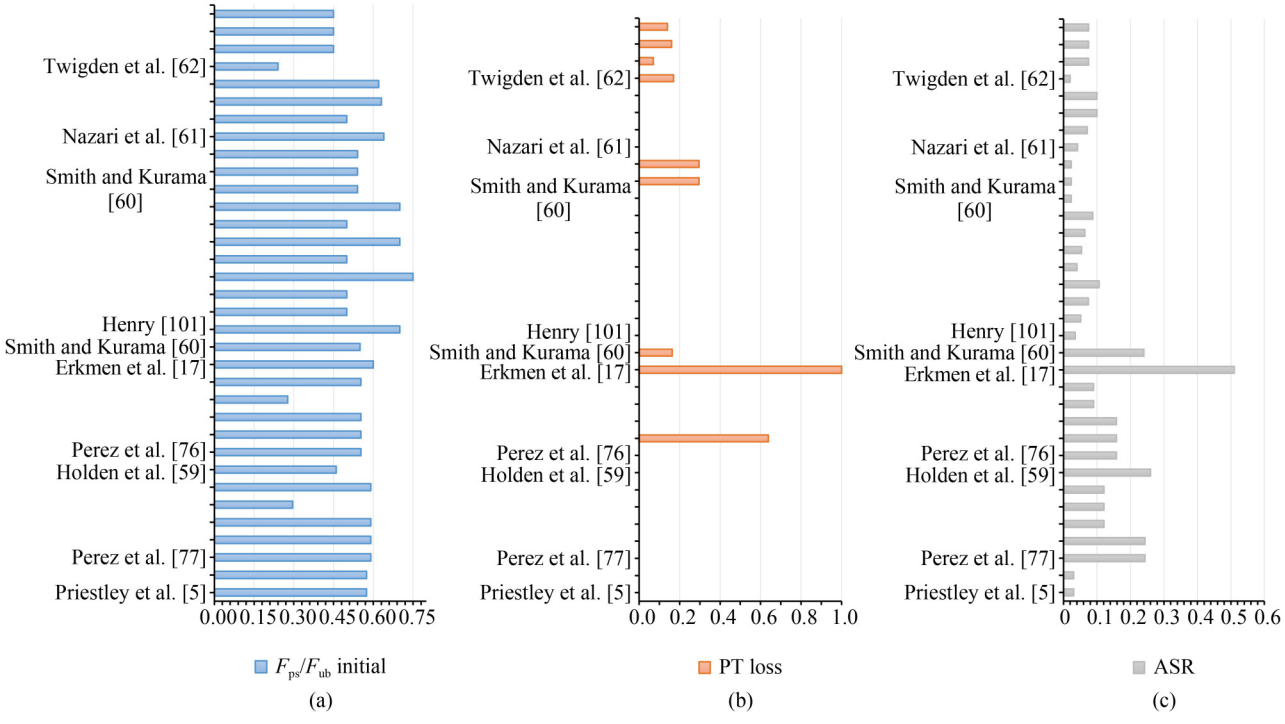

Fig. 18 Concrete wall tests: (a) initial PT stress in tendon to tendon ultimate stress; (b) PT losses; (c) ASR.

considered in this review. The PT stress ratio to the PT strand ultimate strength in the observed masonry walls did not exceed 80% as can be observed in Fig. 19. The PT losses in the ultimate limit state of masonry walls varied from 10% to 90%. It can also be observed that the maximum ASR among observed walls is 17.5%. It is worth mentioning that the PT losses due to long-term shrinkage and creep in ungrouted masonry can reach 20 to 29% and in fully grouted masonry from 25% to 35% having 0.15 ASR and 0.7f_{pu} initial stress [106] where f_{pu} is the ultimate strength of PT bar or strand.

The number of reported tests on PT timber shear walls is limited. Table A2 also includes a list of the tested PT timber walls. Figure 20 presents the initial stress value in the tendon, PT loss and ASR for the PT timber walls. It can be observed that only one out of six walls experience PT loss in the ultimate limit state. The value of the reported PT loss was 12% which is much lower compared to masonry or concrete PT shear walls. The smaller PT loss in timber in comparison to masonry and concrete can be due to timbers experiencing a lower amount of damage when the wall toe pounds on the foundation.

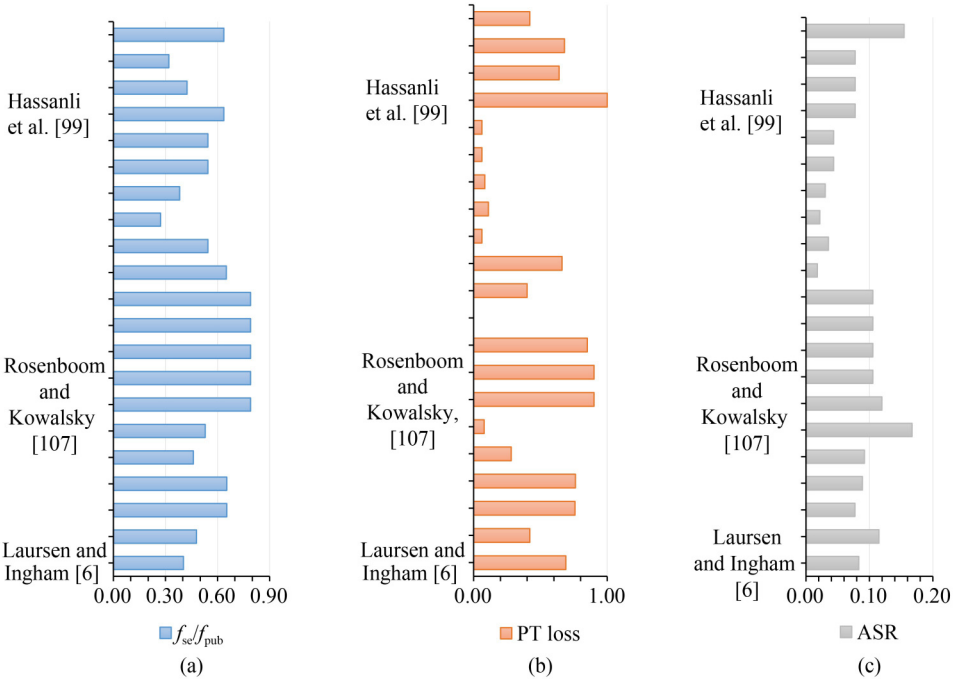

Fig. 19 Masonry wall tests: (a) initial PT stress in tendon to tendon ultimate stress; (b) PT losses; (c) ASR.

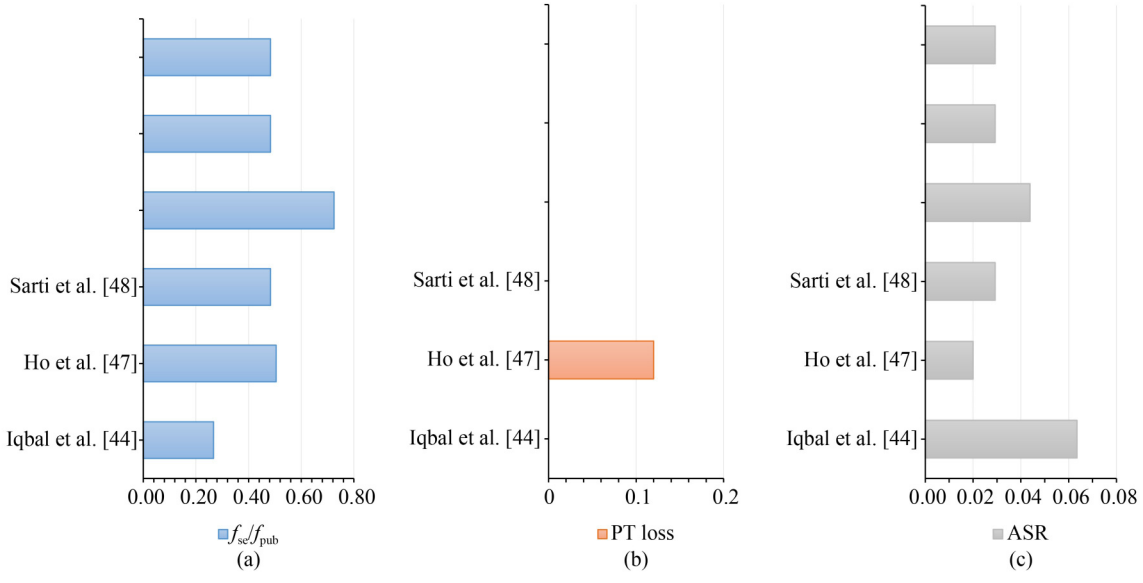

Fig. 20 Timber wall tests: (a) initial PT stress in tendon to tendon ultimate stress; (b) PT losses; (c) ASR.

5 Residual drifts

Self-centering structures are expected to display smaller residual drifts in comparison to monolithic conventional ones, and residual displacement is a critical design aspect of self-centering structures. However, there is no limit considered for the residual drift of self-centering PT walls in standards [20,21]. The contact between the wall panel and the foundation during load reversal can result in damage to wall toes. Steel plates or plastic sheets at the joints between the wall panel and foundation can mitigate the damage due to pounding [108]. Fiber-reinforced concrete can also be used for this purpose [95]. A strong material at wall panel toe or a flexible one that experience less damage during cyclic loads can result in smaller PT losses and lead to better serviceability performance of the wall.

According to performance based seismic design concept, ordinary buildings with conventional structural systems are expected to produce Immediate Occupancy (IO), Life Safety (LS) and near Collapse Prevention (CP) performances when subject to ground motions compatible with earthquake intensities of EQ-I, EQ-II, EQ-III and EQ-IV respectively, for which the earthquake name, year and station is nominated for each intensity by Rahman and Sritharan [109]. At minimum, the precast rocking walls are expected to provide same level of performances (IO/LS/CP). Rahman and Sritharan [109] defined the inter-story drift limits of the joined wall system performances at the four earthquake intensity levels: maximum transient drifts of 0.4% (EQ-I), 1.2% (EQ-II), 2.0% (EQ-III), and 3.0% (EQ-IV) and maximum permissible residual drifts as 0.1% (EQ-I), 0.3% (EQ-II), 0.5% (EQ-III), and 0.75% (EQ-IV).

Henry [101] considered permanent residual drift limit to 0.2% following the design level earthquake (DE) (equivalent to hazard level of EQ-III) and 0.3% following the MCE (equivalent to hazard level of EQ-IV) for preWEC walls. Nazari et al. [61] also considered Rahman and Sritharan [109] recommended limits.

The residual drifts recorded according to experimentally tested concrete PT walls is shown in Fig. 21. The residual drifts are recorded based on the drift value where the hysteresis loop reaches the 0.5% and 2.0% drift and unloaded to zero lateral force [62]. According to Rahman and Sritharan [109], the permissible story drift is 0.4% and 2.0% for EQ-I and EQ-III respectively. It can be observed in Fig. 21 that the upper bound of residual drifts in tested concrete walls at 0.5% and 2.0% cycles are 0.1% and 0.46% respectively. All experimentally tested PT concrete walls have smaller residual drifts compared to the permissible value of 0.1% for EQ-I and 0.5% for EQ-III.

It is important to mention that the calculated residual drifts from pseudo-static load tests do not represent the actual residual drifts the walls would experience in an earthquake [62] due to damping in seismic loads. Thus, to better understand the residual drifts of self-centering PT concrete walls, dynamic tests are required. Nazari et al. [61] tested single panel PT concrete wall using shake table and the residual drifts at 2.0% drift cycle was 0.09% and 0.23% for SRW2 and SRW3 walls.

A parametric study by Jafari et al. [69], as the results are shown in Fig. 22, indicated that increasing the ASR would increase the residual drift. Limiting the ASR to 0.15 which is discussed earlier will result in 0.20% and 0.55% residual drift in LS and CP performance levels respectively.

It is worthwhile to remark that the PT wall lateral stiffness is highly sensitive to ASR. MacRae and Kawashima [110] mentioned that the dynamic residual drift is sensitive to post-yield stiffness of the bilinear

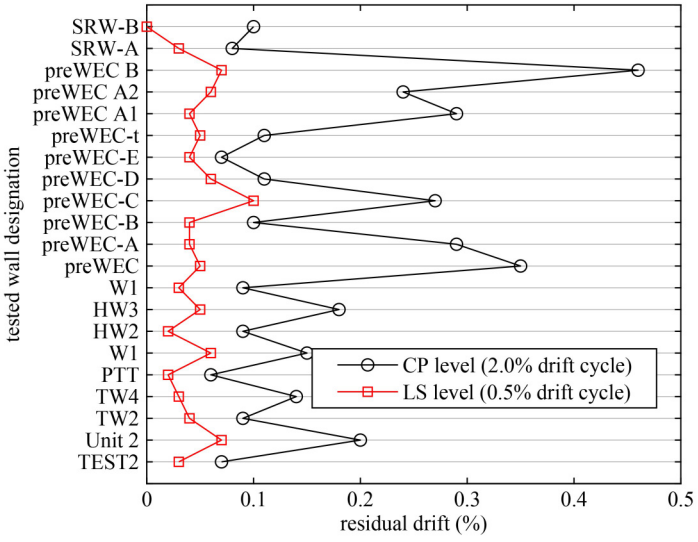

Fig. 21 Residual drifts of PT concrete walls at LS and CP performance levels according to ASCE 7-16 [98].

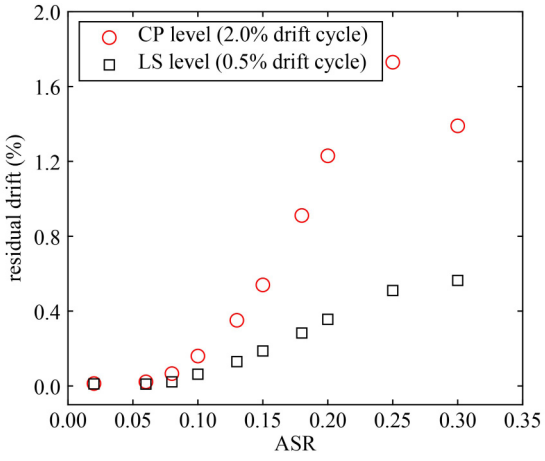

Fig. 22 Residual drift of tested walls.

elasto-plastic hysteresis rule.

The residual drifts of timber and masonry rocking walls are presented in Figs. 23 and 24, respectively, and the reference for wall designations are tabulated in Table A2 [6,44,45,47,48,80,81,107,111,112]. The maximum residual drift as an acceptance criterion would be 0.20% and 0.35% for LS and CP levels for timber rocking walls, respectively. These values would be 0.20% and 0.65% for masonry rocking walls, respectively.

6 Conclusions

This paper critically reviewed the behavior of rocking concrete, masonry and timber shear walls based on the available literature. A database of more than 100 test

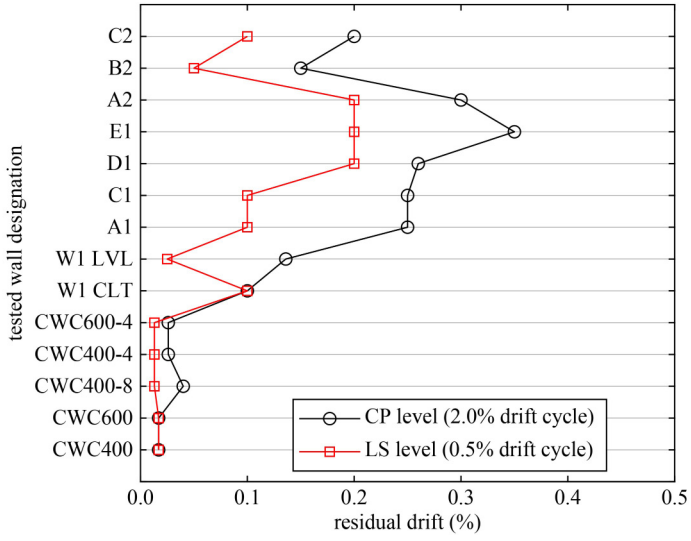

Fig. 23 Residual drifts of PT timber walls at LS and CP performance levels according to ASCE 7-16 [98].

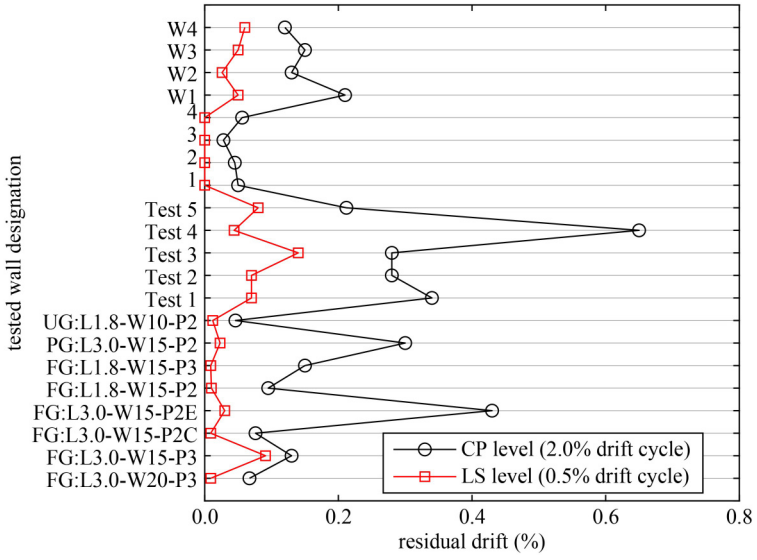

Fig. 24 Residual drifts of PT masonry walls at LS and CP performance levels according to ASCE 7-16 [98].

walls were collected and the walls' configurations, confinement, joints, ED, seismic performance factors, PT loss and residual drifts were examined. The outcomes of this investigation are summarized below.

1) Based on the comparison of the test results of the walls' database, it is recommended to confine the edge of the wall to improve its ductility and avoid premature failure. A minimum volumetric confinement reinforcement ratio of 2.0% is suggested to be used within the $0.08l_w$ of the edge of the wall along the walls' length and $0.40l_w$ along the wall's height. No confinement has been considered for timber walls due to the less brittle nature of the timber material. However, similar confinement level can be considered to improve the behavior such rocking walls.

2) The horizontal shear slip limit between the PT concrete wall and foundation or between the wall panels is recommended to be limited to 1.5 mm. No studies have been considered for the horizontal slip limit for masonry and timber rocking walls, however, until more studies are conducted on this area, the same shear slip limit seems to be applicable to be adopted for masonry and timber rocking shear walls.

3) A mild steel moment ratio (κ_d) of 0.5 to 0.8 can be considered for design of concrete rocking walls (κ_d: is defined as the moment contribution of mild steel divided by the sum of moment contribution of PT strands and gravity loads to resist lateral loads). While no studies have been undertaken on κ_d in masonry and timber walls, a lower bond of κ_d = 0.5 can be adopted for design of such walls.

4) Minimum acceptance design criteria for drift are from 0.9% to 3.0% depending on the wall height and length as per ACI ITG-5.1 for rocking concrete walls. More studies are required to set a limit for masonry and timber walls.

5) The preWEC system configuration is recommended for timber and concrete rocking walls as can possibly meet both the self-centering and ED requirements. This method can also be used for masonry walls as an external ED mechanism.

6) While the ductility of the rocking walls is highly sensitive to changes in ASR, the ASCE 7 seismic code uses the same ductility factor irrespective of the wall ASR. Limited studies have been performed to understand the relation between ductility and ASR in masonry and timber rocking walls.

7) Following equations are recommended for preliminary estimation of the fundamental period (T) and response modification factor (R) of PT concrete walls based on the review of the experimentally tested PT concrete walls:

$$T = 0.032H^{1.03},$$

$$R = 1.02H^{1.03} + 0.32f_p/f'_c, \qquad R < 9$$

$$R = 6.7T^2(\mu/1 + 0.023(\mu - 1)) + 2.9T[\mu/1 + 0.023(\mu - 1)]^{0.5} + 3R < 7,$$

where H is wall height in meters, μ is displacement ductility and (f_p/f'_c) is wall ASR.

More parametric studies are required for masonry and timber rocking walls to develop similar equations. Until further study is available, R = 7.0 can be considered for timber walls. For ungrouted, partially grouted, and fully grouted, post-tensioned masonry walls a R can be taken as 1.5, 2.5, and 3.0, respectively.

According to the literature, a value of C_d = 5, 3.5 and 7.5 is suggested for PT concrete, masonry, and timber rocking walls, respectively. The findings in the review revealed that a minimum value for ASR in rocking PT walls needs to be considered to prevent large C_d values which is not covered by current standards. Alternatively for low levels of ASRs, a larger value of C_d should be considered in the standards to provide a safe design.

Comparing different types of walls, it was found that timber walls showed much lower residual drifts compared to concrete and masonry PT walls. Acceptable residual drifts for all concrete, masonry and timber walls at the LS levels is taken as 0.2% drift.

Notations

PBSD: performance based seismic design
NLTH: non-linear time history
T: fundamental period
C_d: displacement amplification factor
R: response modification factor
μ: ductility
PT: post-tensioning
LVL: laminated Veneer Lumber
ED: energy dissipation
ASR: axial stress ratio
AR: aspect ratio
l_w: wall length
β: energy dissipation ratio
EVD (ξ_{eq}): equivalent viscous damping
ξ_v: viscous damping
ξ_{hyst}: hysteresis damping
κ_d: mild steel moment ratio
CLT: Cross Laminated Timber
Pres-Lam: Prestressed Laminated
PreWEC: Prestressed Walls with End Columns
UFPs: U-Shaped Flexural Plates
TCY: tension-compression yield
δ_m: maximum displacement in a fitted bilinear curve
δ_y: yield displacement in a fitted bilinear curve
R_R: redundancy factor

R_μ: ductility reduction factor
R_s: overstrength factor
V_y: base shear at yield point
V_m: base shear at ultimate strength
T_c: characteristic period of the ground motion defined for soil
f_p: sum of stress due to self-weight and PT force
f_c': concrete compressive strength
H: height of the wall
T_s: secant period
MCE: maximin considered earthquake
Ω_0: system over-strength factor
f_{ub}: breaking stress of PT tendons
A_p: tendon cross section area
IO: Immediate Occupancy
LS: Life Safety
CP: Collapse Prevention
DE: design level earthquake

Funding note Open Access funding enabled and organized by CAUL and its Member Institutions.

Electronic Supplementary Material Supplementary material is available in the online version of this article at https://doi.org/10.1007/s11709-022-0850-0 and is accessible for authorized users.

References

1. Sritharan S, Aaleti S, Henry R S, Liu K Y, Tsai K C. Precast concrete wall with end columns (PreWEC) for earthquake resistant design. Earthquake Engineering & Structural Dynamics, 2015, 44(12): 2075–2092
2. Wilson A W, Wilson A W, Motter C J, Phillips A R, Dolan J D. Seismic response of post-tensioned cross-laminated timber rocking wall buildings. Journal of Structural Engineering (United States), 2020, 146(7): 04020123
3. Lu X, Yang B, Zhao B. Shake-table testing of a self-centering precast reinforced concrete frame with shear walls. Earthquake Engineering and Engineering Vibration, 2018, 17(2): 221–233
4. Lu X, Dang X, Qian J, Zhou Y, Jiang H. Experimental study of self-centering shear walls with horizontal bottom slits. Journal of Structural Engineering, 2017, 143(3): 04016183
5. Priestley M J N, Sritharan S S, Conley J R, Stefano Pampanin S. Preliminary results and conclusions from the PRESSS five-story precast concrete test building. PCI Journal, 1999, 44(6): 42–67
6. Laursen P T, Ingham J M. Structural testing of single-storey post-tensioned concrete masonry walls. Masonry Society Journal, 2001, 19: 69–82
7. Yassin A, Ezzeldin M, Steele T, Wiebe L. Seismic collapse risk assessment of posttensioned controlled rocking masonry walls. Journal of Structural Engineering (United States), 2020, 146(5): 04020060
8. Nylander C. Clamps and Chronology. Leiden: Brill Academic Publishers, 1966, 6: 130
9. Roca P, Lourenço P B, Gaetani A. Historic Construction and Conservation: Materials, Systems and Damage. London: Routledge, 2019
10. Sanabra Loewe M, Capellà Llovera J. The four ages of early prestressed concrete structures. PCI Journal, 2014, 59: 93–121
11. Nakaki S D, Stanton J F, Sritharan S S. An overview of the PRESSS five-story precast test building. PCI Journal, 1999, 44(2): 26–39
12. Kyritsis-Spinoulas M, Vangelatos Z, Vassiliou P, Manolakos D, Delagrammatikas M, Papadopoulou O. Steel clamps from the Acropolis: some old, some new and some digital. In: Proceedings of the 5th International Conference on Corrosion Mitigation and Surface Protection Technologies. Luxor: International Quality, 2016, 11–18
13. Housner G W. The behavior of inverted pendulum structures during earthquakes. Bulletin of the Seismological Society of America, 1963, 53(2): 403–417
14. FEMA 356. Commentary for the Seismic Rehabilitation of Buildings. Washington, D.C.: Federal Emergency Management Agency, 2000
15. Kurama Y, Sause R, Pessiki S. Seismic analysis, behavior, and design of unbonded post-tensioned precast concrete walls. Dissertation for the Doctoral Degree. Bethlehem: Lehigh University, 1997
16. Boroschek R L, Yáñez F V. Experimental verification of basic analytical assumptions used in the analysis of structural wall buildings. Engineering Structures, 2000, 22(6): 657–669
17. Erkmen B, Schultz A E. Self-centering behavior of unbonded, post-tensioned precast concrete shear walls. Journal of Earthquake Engineering, 2009, 13(7): 1047–1064
18. Kurama Y C, Sritharan S, Fleischman R B, Restrepo J I, Henry R S, Cleland N M, Ghosh S K, Bonelli P. Seismic-resistant precast concrete structures: State of the art. Journal of Structural Engineering, 2018, 144(4): 03118001
19. ACI 318-14. Building Code Requirements for Reinforced Concrete. Farmington Hills: American Concrete Institute, 2014
20. ACI ITG-5.1-07. Acceptance Criteria for Special Unbonded Post-tensioned Precast Structural Walls Based on Validation Testing and Commentary. Farmington Hills: American Concrete Institute, 2008
21. ACI ITG-5.2-09. Requirements for Design of Special Unbonded Posttensioned Precast Shear Wall Satisfying ACI ITG-5.1 (ACI ITG-5.2-09) and Commentary. Farmington Hills: American

Concrete Institute, 2009
22. FEMA P695. Quantification of Building Seismic Performance Factors: US Department of Homeland Security. Redwood City: FEMA, 2009
23. Loss C, Tannert T, Tesfamariam S. State-of-the-art review of displacement-based seismic design of timber buildings. Construction & Building Materials, 2018, 191: 481−497
24. Murray E B. Dry Stacked Surface Bonded Masonry-Structural Testing and Evaluation. Dissertation for the Master's Degree. Prove: Brigham Young University, 2007
25. Sokairge H, Rashad A, Elshafie H. Behavior of post-tensioned dry-stack interlocking masonry walls under out of plane loading. Construction & Building Materials, 2017, 133: 348−357
26. Ambrose R, Hulse R, Mohajery S. Cantilevered prestressed diaphragm walling subjected to lateral loading. Brick and Block Masonry (8 th IBMAC) London, Elsevier. Applied Sciences (Basel, Switzerland), 1988, 2: 583−594
27. Curtin W, Howard J. Lateral loading tests on tall post-tensioned brick diaphragm walls. Applied Sciences (Basel, Switzerland), 1988, 2: 595−605
28. Hobbs B, Daou Y. Post-tensioned T-section brickwork retaining walls. Brick and Block Masonry(8 th IBMAC) London, Elsevier. Applied Sciences (Basel, Switzerland), 1988, 2: 665−675
29. Fisher Bah K, Watt P. Structural testing of brick pocket-type retaining walls. In: Proceedings of 10th IB^{2}Mac. Calgary: Masonry Council of Canada, 1994, 441−448
30. Schultz A E, Scolforo M J. Overview of prestressed masonry. Masonry Society Journal, 1991, 10: 6−21
31. Lissel S, Sayed-Ahmed E, Shrive N. Prestressed masonry-the last ten years. In: Proceedings of the 8th North American Masonry Conference. Austin: The Masonry Society, 1999, 599−610
32. Bean J R, Schultz A E. Flexural capacity of post-tensioned masonry walls: Code review and recommended procedure. PTI Journal, 2003, 1: 28−44
33. Bean Popehn J R, Schultz A E, Drake C R. Behavior of slender, posttensioned masonry walls under transverse loading. Journal of Structural Engineering, 2007, 133(11): 1541−1550
34. Ismail N, Schultz A E, Ingham J M. Out-of-plane seismic performance of unreinforced masonry walls retrofitted using post-tensioning. In: Proceedings of 15th International Brick and Block Masonry Conference. Florianopolis: The Federal University of Santa Catarina, 2012, 1−12
35. Ismail N, Ingham J M. Time-dependent prestress losses in historic clay brick masonry walls seismically strengthened using unbonded posttensioning. Journal of Materials in Civil Engineering, 2013, 25(6): 718−725
36. Bean Popehn J R, Schultz A E. Influence of imperfections on the out-of-plane flexural strength of post-tensioned masonry walls. Construction & Building Materials, 2013, 41: 942−949
37. Kohail M, Elshafie H, Rashad A, Okail H. Behavior of post-tensioned dry-stack interlocking masonry shear walls under cyclic in-plane loading. Construction & Building Materials, 2019, 196: 539−554
38. Wight G D, Ingham J M, Wilton A R. Innovative seismic design of a post-tensioned concrete masonry house. Canadian Journal of Civil Engineering, 2007, 34(11): 1393−1402
39. Rosenboom O A, Kowalsky M J. Reversed in-plane cyclic behavior of posttensioned clay brick masonry wall. Journal of Structural Engineering, 787–798
40. ElGawady MA, Ryu D, Wijeyewickrema AC. Seismic behavior of unbonded post-tensioned masonry walls. In: Proceedings of the 10th National Conference on Earthquake Engineering. Anchorage: Earthquake Engineering research institute, 2014
41. Ryu D, Wijeyewickrema A C, ElGawady M A, Madurapperuma M A K M. Effects of tendon spacing on in-plane behavior of posttensioned masonry walls. Journal of Structural Engineering, 2014, 140(4): 04013096
42. Hassanli R, ElGawady M A, Mills J E. Strength and seismic performance factors of posttensioned masonry walls. Journal of Structural Engineering, 2015, 141(11): 04015038
43. Kalliontzis D, Schultz A, Sritharan S. Modelling of a rocking masonry wall with unbonded post-tensioning subjected to shake-table testing. In: Proceedings of the 11th National Conference in earthquake Engineering. Los Angeles: Earthquake Engineering research institute, 2018
44. Iqbal A, Fragiacomo M, Pampanin S, Buchanan A. Seismic resilience of plywood-coupled LVL wall panels. Engineering Structures, 2018, 167: 750−759
45. Moroder D, Smith T, Dunbar A, Pampanin S, Buchanan A. Seismic testing of post-tensioned Pres-Lam core walls using cross laminated timber. Engineering Structures, 2018, 167: 639−654
46. Sarti F, Palermo A, Pampanin S, Berman J. Determination of the seismic performance factors for post-tensioned rocking timber wall systems. Earthquake Engineering & Structural Dynamics, 2017, 46(2): 181−200
47. Ho T X, Dao T N, Aaleti S, van de Lindt J W, Rammer D R. Hybrid system of unbonded post-tensioned CLT panels and light-frame wood shear walls. Journal of Structural Engineering, 2017, 143(2): 04016171
48. Sarti F, Palermo A, Pampanin S. Development and testing of an alternative dissipative posttensioned rocking timber wall with boundary columns. Journal of Structural Engineering, 2016, 142(4): E4015011
49. Loo W Y, Kun C, Quenneville P, Chouw N. Experimental testing of a rocking timber shear wall with slip-friction connectors. Earthquake Engineering & Structural Dynamics, 2014, 43(11): 1621−1639
50. Smith T, Pampanin S, Fragiacomo M, Buchanan A. Design and construction of prestressed timber buildings for seismic areas. In: Proceeding of 10th World Conference on Timber Engineering WCTE 2008. Christchurch: University of Canterbury, 2008
51. Sinha R, Lennartsson M, Frostell B. Environmental footprint assessment of building structures: A comparative study. Building and Environment, 2016, 104: 162−171
52. Pilon D S, Palermo A, Sarti F, Salenikovich A. Benefits of multiple rocking segments for CLT and LVL Pres-Lam wall systems. Soil Dynamics and Earthquake Engineering, 2019, 117: 234−244
53. Jin Z, Pei S, Blomgren H, Powers J. Simplified mechanistic model for seismic response prediction of coupled cross-laminated timber rocking walls. Journal of Structural Engineering, 2019, 145: 04018253

54. Iqbal A, Smith T, Pampanin S, Fragiacomo M, Palermo A, Buchanan A H. Experimental performance and structural analysis of plywood-coupled LVL walls. Journal of Structural Engineering, 2016, 142: 04015123
55. Henry R S, Sritharan S, Ingham J M. Finite element analysis of the PreWEC self-centering concrete wall system. Engineering Structures, 2016, 115: 28−41
56. Guo T, Xu Z, Song L, Wang L, Zhang Z. Seismic resilience upgrade of RC frame building using self-centering concrete walls with distributed friction devices. Journal of Structural Engineering, 2017, 143(12): 04017160
57. Gu A, Zhou Y, Xiao Y, Li Q, Qu G. Experimental study and parameter analysis on the seismic performance of self-centering hybrid reinforced concrete shear walls. Soil Dynamics and Earthquake Engineering, 2019, 116: 409−420
58. Li X, Wu G, Kurama Y C, Cui H. Experimental comparisons of repairable precast concrete shear walls with a monolithic cast-in-place wall. Engineering Structures, 2020, 216: 110671
59. Holden T, Restrepo J, Mander J B. Seismic performance of precast reinforced and prestressed concrete walls. Journal of Structural Engineering, 2003, 129(3): 286−296
60. Smith B, Kurama Y. Seismic behavior of a hybrid precast concrete wall specimen: measured response versus design predictions. In: Proceedings of 9th US National and 10th Canadian Conference on Earthquake Engineering. Toronto: Earthquake Engineering research institute, 2010
61. Nazari M, Sritharan S, Aaleti S. Single precast concrete rocking walls as earthquake force-resisting elements. Earthquake Engineering & Structural Dynamics, 2017, 46(5): 753−769
62. Twigden K M, Sritharan S, Henry R S. Cyclic testing of unbonded post-tensioned concrete wall systems with and without supplemental damping. Engineering Structures, 2017, 140: 406−420
63. Yang B, Lu X. Displacement-based seismic design approach for prestressed precast concrete shear walls and its application. Journal of Earthquake Engineering, 2018, 22(10): 1836−1860
64. Mander J B, Priestley M J, Park R. Theoretical stress−strain model for confined concrete. Journal of Structural Engineering, 1988, 114(8): 1804−1826
65. Masrom M A, Hayati N. Review on the rocking wall systems as a self-centering mechanism and its interaction with floor diaphragm in precast concrete structures. Latin American Journal of Solids and Structures, 2020, 17(6): 1−29
66. Yang B, Lu X. Displacement-based seismic design approach for prestressed precast concrete shear walls and its application. Journal of Earthquake Engineering, 2017, 22(10): 1836−1860
67. NZS 3101. The Design of Concrete Structures. Wellington: Standards New Zealand, 2006
68. ACI 318-R8. Building Code Requirements for Structural Concrete and Commentary. Michigan: American Concrete Institute, 2008
69. Jafari A, Ghasemi M R, Akbarzadeh Bengar H, Hassani B. Seismic performance and damage incurred by monolithic concrete self-centering rocking walls under the effect of axial stress ratio. Bulletin of Earthquake Engineering, 2018, 16(2): 831−858
70. Kam W Y, Pampanin S, Palermo A, Carr A J. Self-centering structural systems with combination of hysteretic and viscous energy dissipations. Earthquake Engineering & Structural Dynamics, 2010, 39: 1083−1108
71. Morgen B G, Kurama Y C. Seismic design of friction-damped precast concrete frame structures. Journal of Structural Engineering, 2007, 133(11): 1501−1511
72. Hassanli R, Youssf O, Mills J E, Karim R, Vincent T. Performance of segmental self-centering rubberized concrete columns under different loading directions. Journal of Building Engineering, 2018, 20: 285−302
73. Twigden K M, Henry R S. Shake table testing of unbonded post-tensioned concrete walls with and without additional energy dissipation. Soil Dynamics and Earthquake Engineering, 2019, 119: 375−389
74. Twigden K. Dynamic response of unbonded post-tensioned concrete walls for seismic resilient structures. Dissertation for the Doctoral Degree. Auckland: The University of Auckland, 2016
75. Smith B, Kurama Y, McGinnis M. Hybrid Precast Wall Systems for Seismic Regions. Structural Engineering Research Report NDSE-2012-01. 2012
76. Perez F J, Sause R, Pessiki S. Analytical and experimental lateral load behavior of unbonded posttensioned precast concrete walls. Journal of Structural Engineering, 2007, 133(11): 1531−1540
77. Perez F J, Sause R, Pessiki S, Lu L W. Lateral load behavior of unbonded post-tensioned precast concrete walls. In: Anson M, Ko J M, Lam E S S, eds. Advances in Building Technology. Oxford: Elsevier, 2002, 423−430
78. Smith B, Kurama Y. Seismic Design Guidelines for Special Hybrid Precast Concrete Shear Walls. Structural Engineering Research Report NDSE-2012-02. 2012
79. Buddika H S, Wijeyewickrema A C. Seismic shear forces in post-tensioned hybrid precast concrete walls. Journal of Structural Engineering, 2018, 144(7): 04018086
80. van der Meer L J, Martens D R W, Vermeltfoort A T. UPT rectangular and flanged shear walls of high-strength CASIEL-TLM masonry: Experimental and numerical push-over analysis. Engineering Structures, 2013, 49: 628−642
81. Hassanli R, ElGawady M A, Mills J E. Experimental investigation of in-plane cyclic response of unbonded posttensioned masonry walls. Journal of Structural Engineering, 2016, 142(5): 04015171
82. Kalliontzis D, Schultz A E. Improved estimation of the reverse-cyclic behavior of fully-grouted masonry shear walls with unbonded post-tensioning. Engineering Structures, 2017, 145: 83−96
83. Laursen P T, Ingham J M. Structural testing of large-scale posttensioned concrete masonry walls. Journal of Structural Engineering, 2004, 130(10): 1497−1505
84. Hossain K, Aaleti S, Dao T N. Experimental investigation and finite-element modeling of an aluminum energy dissipater for cross-laminated timber walls under reverse cyclic loading. Journal of Structural Engineering (United States), 2021, 147(4): 04201025
85. Fitzgerald D, Miller T H, Sinha A, Nairn J A. Cross-laminated timber rocking walls with slip-friction connections. Engineering

Structures, 2020, 220: 110973
86. Hashemi A, Quenneville P. Large-scale testing of low damage rocking Cross Laminated Timber (CLT) wall panels with friction dampers. Engineering Structures, 2020, 206: 110166
87. Amer A, Sause R, Ricles J. Experimental study on self-centering cross-laminated timber shear wall-floor diaphragm sub-assembly. In: Proceedings of International Conference on Advances in Experimental Structural Engineering. Christchurch: University of Canterbury, 2020
88. Lin C P, Wiebe R, Berman J W. Analytical and numerical study of curved-base rocking walls. Engineering Structures, 2019, 197: 109397
89. NZS1170.5. Structural Design Actions Part 5: Earthquake actions—New Zealand. Wellington: Standards New Zealand, 2004
90. ATC-19. Structural Response Modification Factors. ATC Report 19. 1995
91. ATC. Seismic Evaluation and Retrofit of Concrete Buildings. 2 Appendices. Albany: ATC, 1996
92. EC8. Eurocode 8: Design of Structures for Earthquake Resistance—Part 1: General Rules, Seismic Actions and Rules for Buildings. Brussels: European Committee for Standardization, 2005
93. FEMA 440. Improvement of Nonlinear Static Seismic Analysis Procedures. Redwood City: Federal Emergency Management Agency, 2005
94. Watanabe G, Kawashima K. An evaluation of the displacement amplification factors for seismic design of bridges. In: Proceedings of 1st International Conference on Urban Earthquake Engineering. Tokyo: Tokyo Institute of Technology, 2004, 89−96
95. Preti M, Meda A. RC structural wall with unbonded tendons strengthened with high-performance fiber-reinforced concrete. Materials and Structures, 2015, 48(1−2): 249−260
96. Fajfar P. Structural analysis in earthquake engineering—A breakthrough of simplified non-linear methods. In: Proceedings of 12th European Conference on Earthquake Engineering. Oxford: Elsevier, 2002
97. FEMA 369. NEHRP Recommended Provisions for Seismic Regulations for New Buildings and Other Structures, Commentary. Washington D.C.: Federal Emergency Management Agency, 2001
98. ASCE 7-16. Minimum Design Loads and Associated Criteria for Buildings and Other Structures. Virginia: ASCE Reston, 2017
99. Hassanli R, ElGawady M A, Mills J E. Force–displacement behavior of unbonded post-tensioned concrete walls. Engineering Structures, 2016, 106: 495−505
100. Jafari A, Bengar H A, Hassanli R, Nazari M, Dugnani R. The response of self-centering concrete walls under quasi-static loading. Bulletin of Earthquake Engineering, 2021, 19: 2893−2917
101. Henry R S. Self-centering precast concrete walls for buildings in regions with low to high seismicity. Dissertation for the Doctoral Degree. Auckland: The University of Auckland, 2011
102. Elnashai A S, Di Sarno L. Fundamentals of Earthquake Engineering. New York: Wiley, 2008
103. Casagrande D, Pacchioli S, Polastri A, Pozza L. Influence of the rocking behavior of shearwalls on the fundamental period of CLT structures. Earthquake Engineering & Structural Dynamics, 2021, 50(6): 1734−1754
104. Gilbert R I, Mickleborough N C, Ranzi G. Design of Prestressed Concrete to AS3600-2009. Boca Raton: CRC Press, 2016
105. AS 3600. Concrete Structures. Sydney: Standards Australia, 2018
106. Laursen PPT. Seismic analysis and design of post-tensioned concrete masonry walls. Dissertation for the Doctoral Degree Auckland: University of Auckland, 2002
107. Rosenboom O A, Kowalsky M J. Reversed in-plane cyclic behavior of post-tensioned clay brick masonry walls for high performance modular housing. In: Anson M, Ko J M, Lam E S S, eds. Advances in Building Technology. Oxford: Elsevier, 2002, 247−254
108. Hamid N, Mander J B. Lateral seismic performance of multipanel precast hollowcore walls. Journal of Structural Engineering, 2010, 136(7): 795−804
109. Rahman M A, Sritharan S. An evaluation of force-based design vs. direct displacement-based design of jointed precast post-tensioned wall systems. Earthquake Engineering and Engineering Vibration, 2006, 5(2): 285−296
110. MacRae G A, Kawashima K. Post-earthquake residual displacements of bilinear oscillators. Earthquake Engineering & Structural Dynamics, 1997, 26(7): 701−716
111. Smith B J, Kurama Y C, McGinnis M J. Design and measured behavior of a hybrid precast concrete wall specimen for seismic regions. Journal of Structural Engineering, 2011, 137(10): 1052−1062
112. Wight G D. Seismic performance of a post-tensioned concrete masonry wall system. Dissertation for the Doctoral Degree. Auckland: University of Auckland, 2006